ISTANBUL TECHNICAL UNIVERSITY ★ GRADUATE SCHOOL

UTILIZING SOME FOREST BIOMASS AS SUPERCAPACITOR ELECTRODE MATERIAL

M.Sc. THESIS

Yaren BUMİN

Department of Chemical Engineering

Chemical Engineering Programme

JUNE 2025

ISTANBUL TECHNICAL UNIVERSITY ★ GRADUATE SCHOOL

UTILIZING SOME FOREST BIOMASS AS SUPERCAPACITOR ELECTRODE MATERIAL

M.Sc. THESIS

Yaren BUMİN
(506211040)

Department of Chemical Engineering

Chemical Engineering Programme

Thesis Advisor: Prof. Dr. Hanzade AÇMA

JUNE 2025

ISTANBUL TEKNİK ÜNİVERSİTESİ ★ LİSANSÜSTÜ EĞİTİM ENSTİTÜSÜ

ORMAN BİYOKÜTLELERİNİN SÜPERKAPASİTÖR ELEKTROT MALZEMESİ OLARAK KULLANIMI

YÜKSEK LİSANS TEZİ

Yaren BUMİN
(506211040)

Kimya Mühendisliği Anabilim Dalı

Kimya Mühendisliği Programı

Tez Danışmanı: Prof. Dr. Hanzade AÇMA

HAZİRAN 2025

Yaren Bumin, a M.Sc. student of İTU Graduate School student ID 506211040, successfully defended the thesis/dissertation entitled “UTILIZING SOME FOREST BIOMASS AS SUPERCAPACITOR ELECTRODE MATERIAL”, which she prepared after fulfilling the requirements specified in the associated legislations, before the jury whose signatures are below.

Thesis Advisor :	**Prof. Dr. Hanzade AÇMA** İstanbul Technical University	.....
Jury Members :	**Prof. Dr. Serdar Yaman** Istanbul Technical University	.....
	Assc. Prof. Dr. Halit Eren FİGEN Yıldız Technical University	.....

Date of Submission : 30 May 2025
Date of Defense : 23 June 2025

To my little sister,

FOREWORD

As a chemical engineer in the electric automotive industry, I spend most of my time working on battery technologies. I have always been astonished by how fast the developments were being made and lost myself for hours trying to understand them. On the other hand, I wrote my bachelor's degree thesis about sustainability and biomass. I have always enjoyed the laboratory environment and the sense of doing something for the world's benefit. To come up with such a project that includes everything I love working on and yet is unique at the same time has been an exceptionally great adventure.

Firstly, I would like to thank Mustafa Kemal Atatürk for everything he has accomplished for our country; as a woman, I thank him for allowing us to be individuals; and lastly, I thank him for showing what a person should spend their life on what is truly important; I always found comfort in his words: "Persons who know that, that they will not be able to rest along the way when they take a path, will never get tired."

Secondly, I would like to thank my professors, Mrs. Hanzade Açma and Mr. Serdar Yaman, for giving me space and support throughout the project. Their admiration for science has given me a sense of purpose in life that I value above all else. The biggest thanks go to Mr. Anıl Yılmaz, who always helped and guided me through hard, long, and cold laboratory days.

My dear friends Dilge, Nihan, Şevval, and Canberk - were always there to listen and support me every time; thank you for your help and belief in me. My dear boyfriend Eyüp, thank you for your guidance and warmth. To my mother and father, I want to say that I love them and thank them for being there every step of the way. I immensely love my dear Cemre and Atakan, but I dedicate this study to my little sister. Since my bachelor's degree thesis was dedicated to my little brother, it was my sister’s turn.

Yaren BUMİN
(Chemical Engineer)

May 2025
İstanbul

TABLE OF CONTENTS

Page

ABBREVIATIONS

GCV : Gross Calorific Value
NCV : Net Calorific Value
ESS : Energy Storage Systems
CES : Chemical Energy Storage
BES : Battery Energy Storage
FBES : Flow Battery Energy Storage
MES : Mechanical Energy Storage
TES : Thermal Energy Storage
EES : Electrical Energy Storage
SMES : Superconducting Magnetic Energy Storage
EDLC : Electric Double-Layer Capacitors
CNTs : Carbon Nanotubes
AN : Acetonitrile
EV : Electric Vehicles
HTC : Hydrothermal Carbonization
AC : Activated Carbon
CV : Cyclic Coltammetry
GCD : Galvanostatic Discharge
EIS : Electrochemical Impedance Spectroscopy
SEM : Scanning Electron Microscopy
FTIR : Fourier Transform Infrared Spectroscopy
XRD : X-ray Diffraction
XPS : X-ray Photoelectron Spectroscopy
BET : Brunauer-Emmett-Teller

SYMBOLS

C	**:** Capacitance
H	**:** The amount of heat
I	**:** Current
t	**:** Time
V	**:** Voltage
A	**:** Area

LIST OF TABLES

Page

LIST OF FIGURES

Page

UTILIZING SOME FOREST BIOMASS AS SUPERCAPACITOR ELECTRODE MATERIAL

SUMMARY

As energy storage devices, supercapacitors have garnered significant attention due to their high power density, rapid charging capabilities, and long cycle lives. Recent advancements and investments in the electric vehicle industry have driven this growing interest. As a result of this increasing interest and the necessity to reduce dependence on fossil fuels, the search for sustainable sources for electrode coating materials has gained prominence.

In this study, coniferous forest biomasses, specifically Scots pine (Pinus sylvestris), eastern spruce (Picea orientalis), and cedar (Cedrus spp.), were utilized as coating materials. These biomasses were selected for several reasons: their abundant availability in the Northern Anatolia and Mediterranean regions, their potential to contribute to the economy by being converted into high-value-added products, and their ability to support sustainable commercial processes through waste recycling. From a technical perspective, these biomasses were deemed suitable due to their porous carbon structures, ease of synthesis, large surface areas, and environmentally friendly characteristics, in addition to their economic and practical advantages.

This project aims to employ these biomasses as coating materials for supercapacitor electrodes to enhance power density and reduce charge-discharge times. This study seeks to address environmental concerns and further reduce dependence on fossil fuels by using sustainable materials in supercapacitor electrodes. Specifically, the potential of lignocellulosic biomasses from coniferous trees as electrode materials for supercapacitors is being investigated. Using bio-based coating materials from renewable resources presents a sustainable solution for supercapacitor applications.

The primary objective of this research is to develop coating materials from the woody parts of Scots pine, eastern spruce, and cedar to improve the performance of supercapacitors. As part of the project, the woody components of coniferous trees are selected as carbon sources. Elemental and structural analyses of the biomasses are conducted for the interpretation of results. Following physical pretreatment, the biomasses underwent thermal conversion and subsequent activation to prepare them as coating materials. Samples are prepared under varying activation parameters, and comparisons are made among different activation conditions for the same biomass and across different biomasses activated under identical conditions.

Electrochemical measurements are performed to evaluate and compare the samples' performance in enhancing supercapacitor efficiency under different conditions. The optimal conditions for each sample are determined based on the experimental results.

ORMAN BİYOKÜTLELERİNİN SÜPERKAPASİTÖR ELEKTROT MALZEMESİ OLARAK KULLANIMI

ÖZET

Günümüzde enerji depolama teknolojilerinde yaşanan hızlı gelişmeler, sürdürülebilirlik kaygıları ve artan enerji ihtiyacı ile birlikte alternatif enerji depolama çözümlerine olan ilgiyi artırmıştır. Bu bağlamda süperkapasitörler, yüksek güç yoğunlukları, kısa şarj-deşarj süreleri ve uzun çevrim ömürleri sayesinde öne çıkan enerji depolama sistemleri arasında yer almaktadır. Özellikle elektrikli araçlar, yenilenebilir enerji sistemleri ve taşınabilir elektronik cihazlar gibi alanlarda, süperkapasitörlerin kullanımı giderek yaygınlaşmaktadır. Elektrikli araç endüstrisinde yapılan son yatırımlar ve teknolojik gelişmeler, süperkapasitörlerin ticari önemini artırmakta; aynı zamanda sürdürülebilir ve çevre dostu malzemelerin kullanımını da gerekli kılmaktadır.

Süperkapasitörlerin performansında en kritik bileşenlerden biri olan elektrot malzemeleri; cihazın enerji ve güç yoğunluğu, çevrim ömrü ve verimliliği üzerinde doğrudan etkilidir. Geleneksel olarak karbon temelli malzemeler bu amaçla kullanılmakta olup, bu malzemelerin kaynağı, üretim yöntemi ve çevresel etkileri önemli bir araştırma konusudur. Bu bağlamda, elektrot kaplama malzemesi için sürdürülebilir ve yenilenebilir kaynaklara yönelim artmaktadır. Lignoselülozik yapıya sahip orman biyokütleleri, özellikle iğne yapraklı ağaç türleri bu alanda dikkat çekmektedir. Bu çalışma kapsamında kaplama malzemesi olarak sarı çam (Pinus sylvestris), doğu ladini (Picea orientalis) ve sedir (Cedrus libani) gibi Türkiye'nin farklı bölgelerinde yaygın olarak bulunan iğne yapraklı ağaç türlerinin biyokütleleri değerlendirilmiştir.

Söz konusu biyokütlelerin seçilmesinde birçok faktör etkili olmuştur. Öncelikle bu türlerin Kuzey Anadolu ve Akdeniz bölgelerinde doğal olarak yaygın bulunmaları, bu ağaçların biyokütlesinin kolay temin edilebilir olmasını sağlamaktadır. Ayrıca, bu ağaç türlerinin endüstriyel odun üretimi sırasında ortaya çıkan artıklarının değerlendirilmesiyle, atık geri dönüşümüne katkı sağlanması ve bu yolla sürdürülebilir bir döngüsel ekonomi modeline katkı sunulması hedeflenmiştir. Ekonomik ve çevresel avantajlarının yanı sıra, bu biyokütlelerin teknik özellikleri de tercih edilmelerinde etkili olmuştur. Özellikle bu türlerin yüksek karbon içeriği, gözenekli yapı oluşturma potansiyeli, geniş yüzey alanına sahip olmaları ve kimyasal aktivasyon süreçlerine uygunlukları gibi özellikleri, onları süperkapasitör uygulamaları için cazip hale getirmektedir.

Bu çalışmanın temel amacı, söz konusu biyokütlelerin elektrot kaplama malzemesi olarak kullanılmasının süperkapasitörlerin enerji ve güç yoğunluğunu artırmadaki potansiyelini araştırmaktır. Bu bağlamda, biyokütlelerden elde edilen karbon türevlerinin süperkapasitör performansı üzerindeki etkileri sistematik olarak incelenmiştir. Çalışmanın ilk aşamasında, sedir, sarı çam ve doğu ladini odunlarından elde edilen numunelerin kimyasal ve fiziksel yapıları elementel analiz, FTIR (Fourier

Transform Infrared Spektroskopisi), BET yüzey alanı analizi ve diğer karakterizasyon yöntemleriyle detaylı olarak analiz edilmiştir. Elde edilen bu veriler, daha sonraki aşamalarda yapılan elektrokimyasal performans değerlendirmelerinde temel oluşturmuştur.

Biyokütlelerin kaplama malzemesine dönüştürülmesi süreci iki temel aşamadan oluşmaktadır: termal dönüşüm ve kimyasal aktivasyon. İlk olarak, ön işlemden geçirilen biyokütleler karbonizasyon yöntemiyle karbonize edilmiştir. Bu süreç, biyokütlelerin uçucu bileşenlerinin uzaklaştırılmasını ve karbon iskeletinin oluşturulmasını sağlamaktadır. Ardından, karbonize edilmiş numuneler potasyum hidroksit (KOH) ile farklı oranlarda kimyasal olarak aktive edilmiştir. Aktivasyon işlemi, karbon yapının gözenekliliğini ve yüzey alanını artırarak elektrot olarak kullanımda performans artışını sağlamaktadır. Bu bağlamda, her bir biyokütle türü için farklı KOH oranlarında (1:2, 1:3, 1:4) aktivasyon gerçekleştirilmiş ve böylece elde edilen numunelerin karşılaştırmalı değerlendirmesi yapılmıştır.

Elektrot kaplaması olarak hazırlanan numunelerin süperkapasitör performansı, elektrokimyasal yöntemlerle test edilmiştir. Yapılan yapısal analizler sonucu, süperkapasitör malzemesi olarak en uygun numunenin Doğu Ladini olacağını göstermiş ve elektrokimyasal analizler bu biyokütle üzerine yapılmıştır. Bu analizler arasında döngüsel voltametri (CV), galvanostatik şarj-deşarj (GCD), elektroimpedans spektroskopisi (EIS) ve kapasitans hesaplamaları yer almaktadır. Yapılan ölçümler sonucunda, her Doğu Ladini için farklı aktivasyon parametrelerinin süperkapasitör performansına olan etkisi analiz edilmiştir.

Elde edilen bulgular, her bir biyokütle türünün süperkapasitör uygulamaları açısından farklı avantajlara sahip olduğunu göstermiştir. Örneğin, sedir ağacından elde edilen karbonun daha düzenli bir gözenek yapısı sergilediği, sarı çamın ise daha geniş yüzey alanı sağladığı gözlemlenmiştir. Doğu ladini örneklerinde ise hem yüzey alanı hem de elektriksel iletkenlik açısından dengeli bir performans elde edilmiştir. Kimyasal aktivasyon oranlarının artmasıyla birlikte genel olarak özgül kapasitans değerlerinde artış gözlemlenmiş, ancak bu artış belirli bir noktadan sonra doygunluk eğilimi göstermiştir. Bu durum, aktivasyon sürecinde optimum koşulların belirlenmesinin önemini ortaya koymuştur.

Bununla birlikte, bu çalışmada yalnızca kaplama malzemesinin elde edilme süreci değil, aynı zamanda elde edilen malzemenin elektrokimyasal performans üzerindeki doğrudan etkisi detaylı olarak ele alınmıştır. Süperkapasitörlerde hedeflenen yüksek güç yoğunluğu ve düşük şarj-deşarj süresi gibi özelliklerin sağlanabilmesi için, elektrot malzemesinin hem elektriksel iletkenlik hem de iyon geçişine uygun yapıda olması gerekmektedir. Bu nedenle, hazırlanan numunelerin iç yapılarının kontrollü şekilde gözeneklileştirilmesi, karbon yapısının aktivasyon sırasında bozulmadan korunması ve yüzey kimyasının uygun hale getirilmesi, elde edilen sonuçların başarısını doğrudan etkilemiştir. Uygulanan aktivasyon parametrelerinin farklılığı, her biyokütlede özgül kapasitans, direnç ve çevrim kararlılığı gibi temel performans kriterlerinde değişken sonuçlar doğurmuş, bu da her biyokütle numunesi için optimum koşulların ayrı ayrı belirlenmesini zorunlu kılmıştır.

Bu bağlamda çalışma, deneysel bir araştırmanın ötesinde, süperkapasitör uygulamaları için biyokütle tabanlı karbon malzemelerin sistematik değerlendirmesine yönelik bir metodoloji sunmaktadır. Elektrokimyasal karakterizasyonların yanı sıra, her bir aktivasyon yöntemi ve parametresi ile elde edilen yapının yapısal analizlerle desteklenmesi sayesinde, yalnızca en iyi performans gösteren malzeme değil, hangi

yapısal özelliğin hangi elektrokimyasal çıktıyı etkilediğini de ortaya konulmuştur. Böylece bu araştırma, literatürde genellikle göz ardı edilen yapı-performans ilişkisinin detaylı analizine katkı sağlamaktadır.

Gelecekte yapılacak çalışmalarda, farklı karbonizasyon atmosferlerinin (örneğin azot, argon veya CO_2 ortamları), aktivasyon ajanlarının (örneğin H_3PO_4, $ZnCl_2$ gibi) ve post-sentez işlemlerinin (grafenle destekleme, metal oksitlerle kompozit oluşturma vb.) bu biyokütleler üzerindeki etkilerinin araştırılması ile daha yüksek performanslı ve çok işlevli süperkapasitör elektrotları geliştirilmesi mümkündür. Aynı zamanda bu biyokütlelerin endüstriyel ölçekte temini, işlenmesi ve ürünleştirilmesi üzerine yapılacak ekonomik analizler, bu malzemelerin ticari kullanımı için de yol gösterici olacaktır. Bu çalışma, yerli ve doğal kaynakların etkin ve yenilikçi kullanımına yönelik önemli bir adım niteliğinde olup, enerji depolama teknolojilerinde çevreyle uyumlu çözümler geliştirilmesine katkı sağlamayı hedeflemektedir.

Ayrıca bu çalışmada kullanılan biyokütlelerin yerel kaynaklardan temin edilebilir olması, uzun vadede dışa bağımlılığı azaltacak stratejiler açısından da önemlidir. Türkiye gibi orman zenginliği yüksek ülkelerde bu tür biyokütlelerin değerlendirilmesi, yalnızca enerji alanında değil; atık yönetimi, orman endüstrisi yan ürünlerinin değerlendirilmesi ve kırsal kalkınma gibi alanlarda da dolaylı faydalar sağlayabilir. Bu sayede hem ekonomik hem de çevresel açıdan sürdürülebilir bir üretim modeli geliştirmek mümkün olacaktır. Bu malzemelerin yüksek sıcaklıklara dayanıklı olmaları, uzun çevrim ömrü sunmaları ve hızlı enerji geri kazanımı sağlamaları, onları hibrit enerji sistemlerinde de potansiyel aday hâline getirmektedir. Örneğin süperkapasitörler, pil sistemleriyle birlikte kullanıldıklarında hem ani güç taleplerini karşılayabilir hem de pilin ömrünü uzatarak sistemin genel verimliliğini artırabilir.

Bu bağlamda, çalışmanın bir diğer katkısı da süperkapasitör teknolojilerinin sadece laboratuvar ölçekli akademik projelerde değil, aynı zamanda gerçek hayat uygulamaları için de ölçeklenebilir malzeme ve yöntem önerileri sunmasıdır. Özellikle elektrikli araç teknolojilerinde batarya sistemlerine destek olarak kullanılan süperkapasitörler, ani hızlanma ve rejeneratif frenleme gibi yüksek güç gereksinimi olan durumlarda önemli rol oynamaktadır. Geliştirilen bu biyokütle temelli kaplama malzemeleri, söz konusu uygulamalarda ticari karbonlara alternatif olarak değerlendirilebilecek seviyeye ulaşmıştır. Bu açıdan çalışmada elde edilen sonuçlar, hem akademik bilgi birikimine katkı sağlamakta hem de sektörel uygulamalara geçiş için bir temel oluşturmaktadır.

Bu tür araştırmaların bir diğer önemi de, fosil yakıtlara dayalı geleneksel elektrot üretim süreçlerinin hem ekonomik hem de çevresel açıdan sürdürülebilir olmamasıdır. Bu nedenle, biyokütle temelli karbon malzemelerin değerlendirilmesi yalnızca teknik performans açısından değil, aynı zamanda sürdürülebilirlik, yerel kaynak kullanımı ve atık yönetimi gibi çok boyutlu kazanımlar sunmaktadır. Özellikle orman endüstrisinde sıklıkla ortaya çıkan artıkların yüksek katma değerli ürünlere dönüştürülmesi, hem çevresel yükün azaltılması hem de kırsal kalkınmanın desteklenmesi açısından önem arz etmektedir. Bu çalışmada kullanılan sedir, doğu ladini ve sarı çam örnekleri, yalnızca teknik olarak başarılı karbon yapılar sunmakla kalmamış, aynı zamanda döngüsel ekonomi açısından da umut vaat eden sonuçlar ortaya koymuştur.

Yapılan karakterizasyon ve elektrokimyasal testler sonucunda elde edilen veriler, her bir biyokütlenin farklı aktivasyon parametrelerine verdiği tepkilerin değişken olduğunu ortaya koymuştur. Bu bağlamda yalnızca materyalin kimyasal bileşimi değil, aynı zamanda gözenek dağılımı, yüzey alanı, karbonizasyon sıcaklığı ve aktivasyon oranı gibi birçok parametrenin optimize edilmesi gerektiği anlaşılmıştır. Örneğin sarı çam, daha düşük sıcaklıklarda karbonize edilmesine rağmen yüksek yüzey alanı ve gözeneklilik özellikleri sayesinde yüksek kapasitans değerlerine ulaşırken, sedir odunu daha düzenli bir karbon yapısı sergileyerek döngüsel kararlılık açısından öne çıkmıştır. Doğu ladini ise, bu iki özellik arasında dengeli bir performans sunarak hem enerji yoğunluğu hem de çevrim ömrü açısından tatmin edici sonuçlar vermiştir.

Sonuç olarak, bu çalışma yalnızca laboratuvar ölçeğinde performans değerlendirmesi yapmakla kalmayıp, aynı zamanda bu tür biyokütle kaynaklarının endüstriyel üretim süreçlerine entegrasyon potansiyelini de göz önünde bulundurmuştur. Özellikle gelecekte süperkapasitör üretiminde karbon izinin azaltılması, sürdürülebilirlik kriterlerinin sağlanması ve yerli kaynakların değerlendirilmesi açısından bu tür malzemelerin büyük katkı sağlayabileceği öngörülmektedir. Elde edilen veriler ışığında, farklı aktivasyon teknikleriyle desteklenen biyokütle kaynaklarının, performans kaybı olmaksızın konvansiyonel karbon bazlı elektrotlara alternatif olabileceği değerlendirilmiştir. Bu doğrultuda, ileriye dönük çalışmalarda biyokütle çeşitliliğinin artırılması, pilot üretim ölçeklerine geçilmesi ve cihaz seviyesinde entegrasyon çalışmalarına başlanması önerilmektedi

1. INTRODUCTION

Due to their high energy densities, fossil fuels remain the primary energy source globally. However, greenhouse gases released during their processing in power plants account for 35% of the world's total greenhouse gas emissions [1]. Additionally, coal-fired power plants in China are responsible for 42% of nitrous oxide emissions and 38% of sulfur dioxide emissions, underscoring their significant contribution to global warming [2]. In 2018 alone, over 300 natural disasters occurred due to climate change, affecting 68 million people and resulting in an estimated economic loss of $131.7 billion [3]. Considering projections that energy demand will increase by 56% by 2040, the urgency of finding alternatives to fossil fuels is becoming increasingly critical [4]. To address this need, this study focuses on biomass, which emerges as a sustainable solution. Biomass encompasses all plant-derived organic materials, including trees, crops, and algae. It comprises terrestrial and aquatic vegetation and all organic waste formed through the photosynthetic process by which green plants convert sunlight into plant matter [5]. From an energy perspective, organic waste, often regarded as “waste,” can instead be seen as a valuable “resource.” As an energy source, biomass is humanity’s oldest fuel, with wood being used for cooking and heating for over 500,000 years. The primary conversion methods for biomass into high-value-added products, depending on the temperature range applied, include hydrothermal carbonization (180–250 °C), torrefaction (200–300 °C), slow pyrolysis (carbonization, 300–450 °C), fast pyrolysis (500–800 °C), gasification (800–1000 °C), and high-temperature steam gasification (>1000 °C) [6]. In this project, a temperature of 900 °C was employed, focusing on the use of biomass in supercapacitor applications. Supercapacitors are utilized in applications requiring rapid storage and discharge of large amounts of energy, such as hybrid, electric, and fuel cell vehicles. For instance, in modern electric vehicles, the engine shuts down completely when the vehicle stops and efficiently restarts using energy stored in supercapacitors. Over 600 electric vehicle applications use supercapacitors in stop-start systems [7]. However, supercapacitors used in commercial applications face disadvantages such as low energy densities and high

production costs [8]. For these reasons, producing supercapacitors from renewable and sustainable carbon sources will provide significant economic benefits and be a highly sought-after alternative.

1.1 Purpose of Thesis

Supercapacitors are energy storage devices that have gained much attention because of their high power density, fast charging and discharging, and long cycle life. Especially given the recent advancements and investments that have been made in the electric vehicle sector, there has been increasing interest in supercapacitors [9]. The paper seeks to identify sustainable materials for supercapacitor electrodes to mitigate the adverse effects of electricity generation on the environment and reduce reliance on fossil fuels. In this regard, it examines the possibility of using tree woods as a viable source of lignocellulosic biomass for supercapacitor electrode materials.

1.2 Hypothesis

Forest biomass is a ready production available carbon-based replenishable materials resource that has the potential to be used excellently in electrochemical properties for supercapacitor applications. Pyrolysis and activation processes can enhance the forest biomass structure and composition to have a large surface area, high electrical conductivity, and stability [10]. It holds great promise to offer a green and sustainable solution for electrode materials, which would help advance energy storage systems with low environmental concerns.

2. THEORY

2.1 Chemical Properties

Biomass is a heterogeneous class of organic materials, primarily composed of cellulose, hemicellulose, and lignin [11,5]. The chemical composition of biomass varies with its source and type, affecting its processing and uses [11]. Some important properties include moisture content, calorific value, fixed carbon to volatile matter ratios, ash content, alkali metal concentrations, and cellulose to lignin ratio [11,6].

Moisture content is an important parameter in inherent and extrinsic forms [6]. Intrinsic moisture is inherent to biomass, while extrinsic moisture depends on the surrounding environment; the latter prevails in practical uses [6]. The calorific value refers to the energy stored in biomass, measured as the heat of combustion. It is expressed in terms of gross calorific value (GCV) or net calorific value (NCV) [5]. Dry and ash-free biomass typically has a fixed energy content of 17–21 MJ/kg [11,5]. The proportions of fixed carbon and volatile matter also strongly influence thermal conversion. Volatile matter, given off as gas on heating, contrasts fixed carbon, which remains a solid residue [6]. Ash content, the non-combustible solid residue, is also an important factor because high ash content could make the processing difficult. Alkali metals like sodium and potassium may combine with silica in the ash, creating operational problems during thermal treatment. The cellulose-to-lignin ratio is significant for biochemical conversion since cellulose is more biodegradable than lignin [5].

The composition of biomass varies between different types [11,5]. Woody biomass, such as pine and plywood, has tightly bound fibers, slow growth, and high lignin content [11]. Herbaceous biomass, including miscanthus and switchgrass, has loosely bound fibers, lower lignin content, and higher ash levels [11,5]. Aquatic biomass, such as seaweed, has a variable composition: brown seaweed is high in carbohydrates, and red seaweed contains more protein [12]. These chemical characteristics will determine the processing methods for biomass directly: Dry biomass conversion pays more

attention to moisture content, calorific value, fixed carbon, volatile matter, ash, and alkali metals, while wet biomass conversion pays more attention to moisture content and cellulose-to-lignin ratio [5].

Various thermochemical processes are applied to convert biomass. Pyrolysis is the thermal decomposition that converts biomass into bio-oil, syngas, and biochar. Studies have shown that biochar has a high calorific value because of the increased fixed carbon concentration. Efficiency in pyrolysis is controlled by several factors that range from moisture content to particle size, ash content, and volatile matter content, among other parameters like reactor type, temperature, and heating rate [10]. Modeling of pyrolysis of biomass materials, including pine, cellulose, hemicellulose, and lignin, has been done to understand the different stages, time scales, and products formed from these chemical reactions [11]. For example, an autocatalytic model has been developed for the secondary degradation pathways of pine pyrolysis [6].

Gasification is a thermochemical process that converts biomass into synthesis gas, a mixture of hydrogen, carbon monoxide, and other gases. Syngas can be used for power generation or as a feedstock for chemical synthesis. The gasification process depends upon the chemical composition of biomass, the gasification medium, the temperature at which the process is conducted, and the reactor type used. Fixed-bed, fluidized-bed, and entrained-flow are a few types of gasifiers. In addition to these methods, supercritical water gasification treats wet biomass under higher temperatures and pressure [6].

Biochar is a carbon-rich solid obtained from the thermochemical conversion of biomass. It has a higher calorific value than the parent material and can be used as a soil amendment or as fuel [6]. These various conversion routes provide ways to optimize the use of biomass and develop a circular economy [10].

Wood biomasses are lignocellulose, which is comprised of cells made up of cellulose, hemicellulose, and lignin [3,4]. Besides Lignin, Hemicelluloses, and Cellulose, which are significant components of biomass, elemental components such as carbon, hydrogen, oxygen, sulfur, and nitrogen are the other components of lignocellulosic biomasses that determine the fuel quality of biomass [5]. The percentage of these components in biomass depends on biomass species. However, studies have shown that lignocellulosic biomass contains about 49% carbon, 6% hydrogen, 44% oxygen, and between 0.1% and 0.5% nitrogen content [5]. Fixed carbon, ash content, volatile

matter, and moisture content are parameters of the proximate composition of biomass and are, therefore, of fundamental importance to biomass energy use [6].

2.2 Structural Properties

Woody biomass's structural properties are shaped by its hierarchical organization, which ranges from the macroscopic arrangement of tissues to the microscopic configuration of its chemical components. These properties influence woody biomass's mechanical strength, porosity, and overall functionality in various applications [13].

The bark is a protective outer layer composed of dead cork cells and living phloem and plays a role in defending against environmental stresses and pathogens. Sapwood is the outer, living portion of the wood that conducts water and nutrients. It is characterized by high porosity and a higher moisture content than heartwood. Heartwood, the inner, non-living core, provides structural support and is often denser and more resistant to decay due to the accumulation of lignin and extractives. These distinctions in tissue types contribute to woody biomass's mechanical and functional diversity [14].

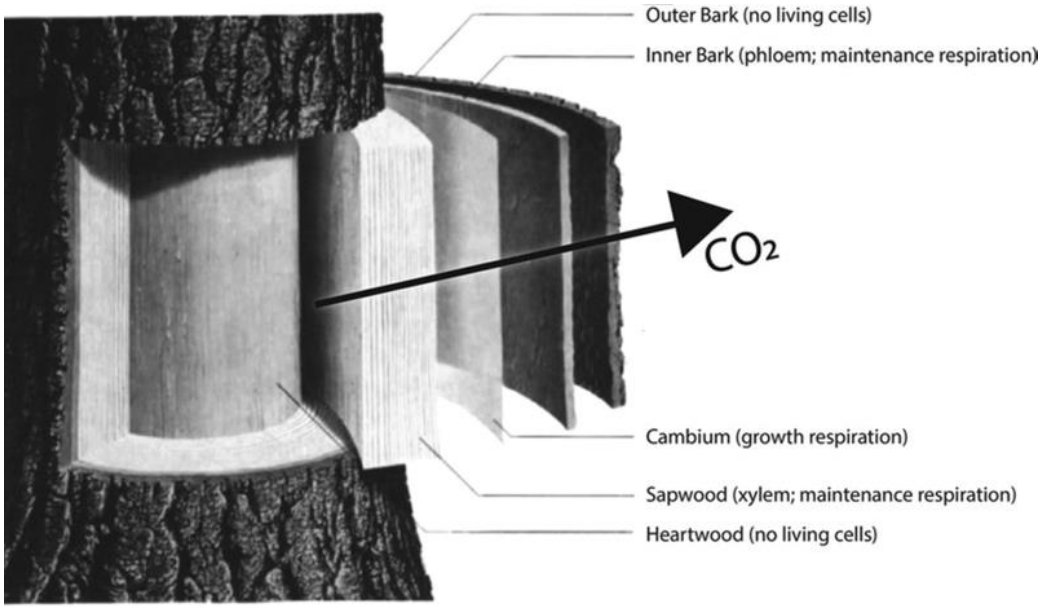

Figure 2.1 : Woody biomass structure [14].

On a microscopic scale, woody biomass is primarily composed of fibers, vessels, and ray cells, creating its porous and anisotropic structure. Fibers of long, slender cells with thick cell walls provide tensile strength and rigidity. Vessels, on the other hand, are larger, hollow cells that form conduits for water transport in hardwood species, while softwoods rely on tracheids for similar functions. Ray cells are radially oriented parenchyma cells that facilitate the lateral transport of nutrients and storage of energy reserves. The arrangement and proportion of these cell types vary across species and directly influence the density, porosity, and mechanical properties of the wood [15].

At the nanoscale, the structural framework of woody biomass is based on its primary chemical components: cellulose, hemicellulose, and lignin. Cellulose microfibrils, composed of highly ordered crystalline regions interspersed with amorphous zones, are embedded in a matrix of hemicellulose and lignin. The cellulose provides tensile strength, while hemicellulose serves as a flexible binding agent that interacts with both cellulose and lignin. Lignin, as the hydrophobic and amorphous component, fills the spaces between fibers, enhancing rigidity and resistance to compression. This nanoscale composite structure imparts wood with remarkable strength-to-weight ratio and resilience under mechanical loads [16].

Density and porosity are also vital structural properties. The density of woody biomass varies between species and within different parts of the same tree, generally ranging from 440 to 650 kg/m^3 [17]. Higher density correlates with greater mechanical strength and durability but may reduce permeability. Porosity, defined by the volume fraction of voids within the biomass, influences fluid transport and thermal conductivity. Porous structures are particularly advantageous for applications such as biochar production and the development of activated carbons for filtration or energy storage [18].

Additionally, the hierarchical structure of woody biomass provides it with a high specific surface area, which can be further enhanced by chemical and physical treatments. This property is especially relevant in applications such as the production of supercapacitor electrodes, where a high surface area facilitates charge storage. Modifications like pyrolysis or chemical activation can introduce micro- and mesopores, increasing the accessibility of the internal surface [19].

In conclusion, the structural properties of woody biomass, from its macroscopic tissue organization to its nanoscale composite structure, define its functionality and versatility. Its combination of strength, porosity, and anisotropy makes it suitable for a wide range of applications, including bioenergy production, material science, and advanced technologies such as energy storage systems.

3. LITERATURE REVIEW

3.1 Introduction to Energy Storage Technologies

The two primary causes of the rise in energy and power consumption over the past few decades are the world's population growth and changes in consumer behavior. The transportation, construction, and industrial sectors account for a sizable portion of overall energy consumption. Global primary energy consumption increased over twofold, from 270.5 EJ in 1978 to 580 EJ in 2018, and is expected to increase even more by 2060 in all scenarios [20]. This demand causes environmental concerns since the primary energy source is fossil fuels. Hence, using clean and renewable energy sources and employing energy-efficient techniques in energy production and consumption processes is becoming more critical day by day. As a result, all nations are shifting toward sustainable energy sources [21]. In order to address the energy needs of transportation, cleaner transportation solutions must be developed, as vehicle emissions are a significant concern. The use of electric energy will be essential to achieving this objective. Since energy produced from renewable sources depends on the environment, energy storage is essential. Energy can be stored using energy storage systems (ESSs), which can be grouped as follows: chemical, electrochemical, electrical, mechanical, and thermal energy, as can be seen in Figure 3.1 [22].

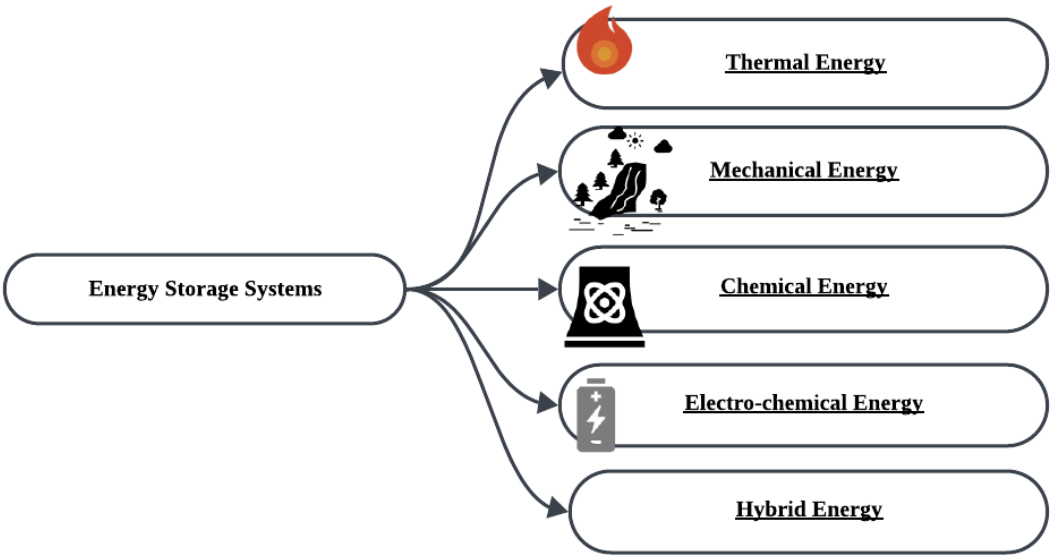

Figure 3.1 : Energy storage systems [22].

3.2 Chemical Energy Storage Systems

Chemical energy storage (CES), such as biomass, coal, and gas, is crucial for the current energy system. It will be an important component of the future renewable energy system globally. Chemical energy storage facilities have the highest capacity, ranging in terawatt-hours [23]. This energy is stored within the chemical bonds of atoms and molecules, and it is released through chemical reactions. During this process, the materials undergo compositional changes as the original bonds break and new ones form [24]. Currently, chemical fuels play a dominant role in both electricity generation and the global transportation sector. Common chemical fuels include coal, gasoline, diesel, natural gas, liquefied petroleum gas (LPG), propane, butane, ethanol, and hydrogen. These fuels are initially converted into mechanical energy, which is then transformed into electrical energy for electricity generation [25]. While we succeed at converting chemical bonds into free electrons, we struggle with the opposite process. This presents the fundamental challenge of chemical energy conversion [26].

3.3 Electrochemical Energy Storage Systems

Electrochemical energy storage devices are typically classified into two types. The first group includes battery energy storage (BES) systems, in which charge is held directly inside the electrodes, and flow battery energy storage (FBES) systems, in which charge is initially stored in the fuel and then moved externally to the electrode surfaces [22]. Beyond these conventional energy storage methods, significant research efforts are focused on advancing electrochemical storage technologies to address the increasing demand for lightweight, compact, and flexible electronic devices.

3.4 Mechanical Energy Storage Systems

Mechanical energy storage (MES) systems store energy by converting it between mechanical and electrical forms. During periods of low demand, such as off-peak hours, electrical energy supplied by the power source is transformed into mechanical energy, which is then stored either as potential energy or kinetic energy [27].

3.5 Thermal Energy Storage Systems

Thermal energy storage (TES) systems are specifically designed to retain heat energy through processes such as cooling, heating, melting, solidifying, or vaporizing of a substance [28]. Based on the operational temperature range, these materials are maintained at high or low temperatures within an insulated container. The stored energy is subsequently recovered and utilized for a wide range of residential and industrial purposes, including space heating or cooling, hot water production, and electricity generation [22]. TES systems are employed across diverse applications, such as industrial cooling below –18 °C, building cooling within the range of 0 to 12 °C, building heating between 25 and 50 °C, and industrial heat storage at temperatures exceeding 175 °C [29].

3.6 Electrical Energy Storage Systems

Electrical energy storage (EES) systems store energy directly in an electric field without converting it into other energy forms. These systems can be categorized as electrostatic energy storage systems and magnetic energy storage systems. Electrostatic energy storage systems include capacitors and supercapacitors while

superconducting magnetic energy storage (SMES) systems fall under the category of magnetic energy storage [22].

A capacitor consists of two metal plates separated by a dielectric layer that does not conduct electricity. When one plate is charged with electricity from a direct-current source, the second plate receives an opposing charge [30]. Metalized plastic films and electrodes can store energy on their surfaces. Capacitors have limited energy density and can only provide or take strong currents for brief periods [31].

3.7 Historical Background

Hermann von Helmholtz, a German physicist, first described the double layer effect [32]. He discovered that a charged electrode immersed in an electrolyte repels ions with the same charge and attracts ions with the opposite charge [33]. In Figure 3.2, first block shows what he represented as the phenomena of a typical capacitor with a charge separation distance H, equal to the radius of the solvated ions. The proposal's fundamental flaw is its assumption that capacity is independent of voltage, which contradicts real-world data [34].

Following this study, Guoy and Chapman separately devised a two layer model that accounts for ion mobility. Ion mobility is governed by a mixture of statistical diffusion and electrostatic forces, as they constitute a danger to point charges [33]. Figure 3.2, second block suggests a diffuse layer in the electrolyte area near the electrodes. Guoy and Chapman's estimated capacity estimates for ions are bigger than actual observations due to their limited size and inability to approach the surface randomly [34].

Stern [35] proposed a double layer that combines the Helmholtz and Guoy-Chapman models, as seen in third block of Figure 3.2. He proposed two types of electrode layers: a compact layer with immobile ions tightly adhered to the surface, akin to the Helmholtz layer, and a diffuse layer with mobile ions using the Guoy-Chapman model [33].

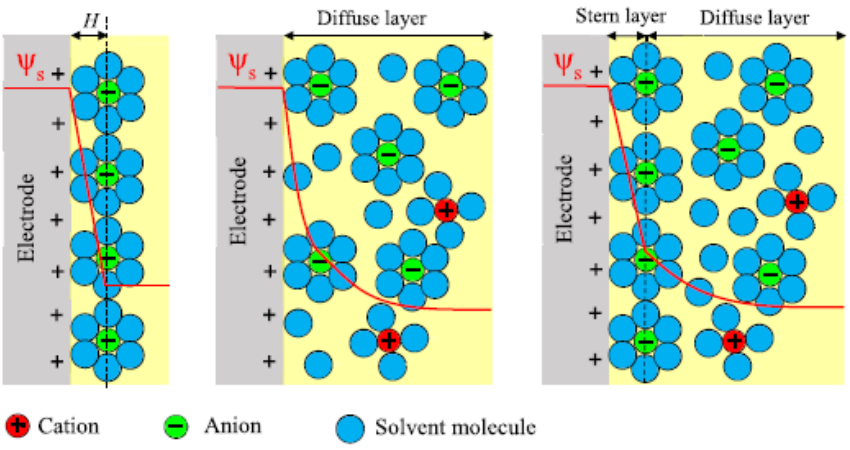

Figure 3.2 : Schematics of the electric double layer structure showing the arrangement of solvated anions and cations close to the electrode - electrolyte interface in the Stern layer and the diffuse layer [32].

In the 1960s, the Standard Oil Company in Cleveland, Ohio (SOHIO) developed the first cell with two layers of activated charcoal. This technology led to the development of modern double-layer capacitors [36].

Since 2007, the focus has shifted toward the development of hybrid supercapacitors. These devices aim to achieve higher nominal voltage, volumetric energy density, and gravimetric energy density compared to traditional electric double-layer capacitors (EDLC). Today, numerous supercapacitors are available with capacitances exceeding thousands of farads and charge-discharge currents ranging from fractions of an ampere to several amperes [7]. These devices provide significant advantages, particularly in scenarios that require high currents, when compared to regular batteries. This capability allows supercapacitors to bridge the gap between batteries and conventional capacitors in energy storage applications. Supercapacitor technology continues to evolve, enabling the production of devices with higher energy density, power output, cycle stability, and operational voltage range. These advancements have expanded their application scope to include hybrid and electric vehicles, portable electronic devices, energy harvesting systems, and power backup solutions [37].

3.8 Key Components of Supercapacitors

Supercapacitors are energy storage devices distinguished by their high power density, rapid charge-discharge cycles, and long lifespan [8]. Fundamentally, they consist of two electrodes, an electrolyte, and a separator as can be seen in 3.4 [38].

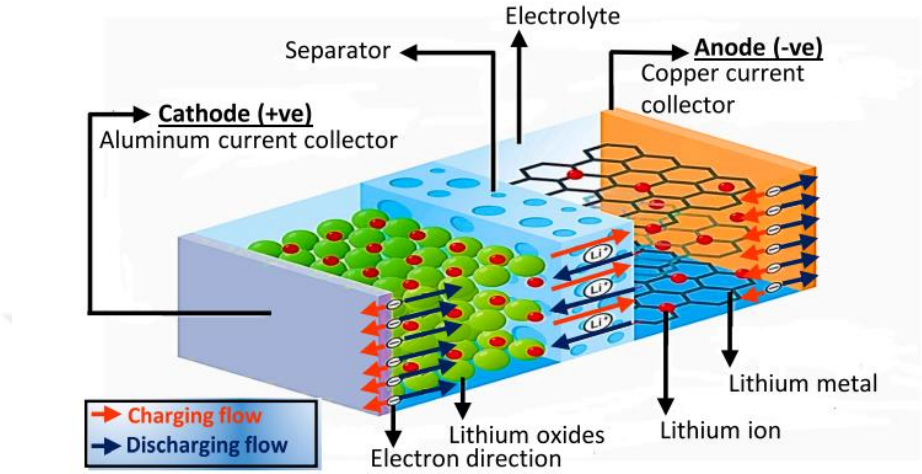

Figure 3.3 : Classification of electrochemical energy storage system [38].

3.9 Electrodes

A critical component influencing their performance is the electrode material. Porous carbon materials with high surface areas are predominantly used due to their excellent electrical conductivity and cost-effectiveness. Below mentioned some electrode coating materials used in applications besides biomass.

Activated Carbon is widely utilized in supercapacitor electrodes because of its high surface area, low cost, and good electrical conductivity. Its porous structure facilitates efficient charge storage, making it a staple in commercial supercapacitors [39].

Carbon Nanotubes (CNTs) are nano-scale carbon materials that offer excellent electrical conductivity, high mechanical strength, and a large surface area. These properties make CNTs suitable for enhancing the performance of supercapacitor electrodes [40]. Graphene is a two-dimensional form of carbon that is just one atom thick, offering remarkable surface area and electrical conductivity. These properties make it a strong candidate for supercapacitor applications, as it can greatly improve energy storage capacity and the rates of charging and discharging [41].

3.10 Electrolytes

The electrolyte in a supercapacitor facilitates ionic conductivity between the electrodes, enabling essential electrochemical reactions. The choice of electrolyte significantly impacts the operating voltage, temperature range, and lifespan of the device. Supercapacitor electrolytes are categorized into three main types: aqueous, organic, and ionic liquids. Aqueous electrolytes, such as KOH and Na_2SO_4 solutions, are valued for their low cost and high ionic conductivity but are limited by a narrow operating voltage range [42]. Organic electrolytes, typically composed of organic solvents like $TEABF_4$ in acetonitrile (AN), offer a broader voltage range but are more expensive and have lower ionic conductivity [43]. Ionic liquids, which are salts that remain liquid at room temperature, provide a wide electrochemical window, high thermal stability, and non-flammability, making them promising for advanced applications. However, their high viscosity and cost present significant challenges [44].

3.11 Separator

The separator in a supercapacitor is crucial because it electrically insulates the two electrodes to prevent short circuits, while still allowing ions to move through. It also needs to have high electrochemical stability to guarantee the longevity and performance of the device. Commonly employed separator materials include porous polymeric films, such as polypropylene and polyethylene, as well as glass fiber-based materials [45].

3.12 Current Collectors

Current collectors are vital conductive elements in supercapacitors, tasked with transferring current from the electrodes to the external circuit. Materials such as aluminum, copper, and stainless steel are commonly used because they offer excellent electrical conductivity and mechanical stability. The resistance of these current collectors plays a crucial role in the power performance of the supercapacitor; higher resistance can lead to energy losses and reduced efficiency [46].

3.13 Types of Supercapacitors

Supercapacitors are categorized into two main types based on their energy storage mechanisms. The first group is Electrochemical Double-Layer Capacitors (EDLCs), which operate on the principle of electrostatic charge accumulation at the electrode-electrolyte interface. The second group is Pseudocapacitors, and they store energy through Faradaic reactions using pseudo-capacitive materials such as metal oxides, conducting polymers, and intercalation compounds [45].

3.14 Factors Influencing Supercapacitor Performance

The distribution of pore sizes in electrodes plays a crucial role in how easily electrolyte ions can reach the electrode surface, which in turn impacts ionic conductivity. A well-designed pore system enhances ion transport efficiency, which in turn boosts the performance of supercapacitors. Studies show that achieving the right balance between the sizes of carbon pores and the electrolyte ions can significantly increase capacitance, highlighting the need to customize pore structures according to the specific properties of the electrolyte. [47].

Additionally, research indicates that the charging rate in supercapacitors is influenced by the speed at which ions can access and settle on the surface of the electrodes [48].

Therefore, controlling the pore size distribution is essential for designing electrodes that maximize ionic conductivity and overall supercapacitor performance.

Furthermore, the functional groups found on the surface of electrodes play a crucial role in electrochemical reactions, particularly in the processes of ion adsorption and desorption. Additionally, these functional groups can influence the wettability of the electrode, which is vital for optimal interaction with the electrolyte. The wettability of electrode materials in relation to the electrolyte significantly affects their electrochemical performance [49].

The wettability of electrode materials with electrolytes in liquid systems is vital for electrochemical energy storage and conversion. Enhancing the wettability of electrodes can facilitate better ion diffusion and expand the ion-accessible surface area, which in turn boosts specific capacity, rate performance, and cycle stability [50].

Therefore, understanding and controlling the surface functional groups and wettability of electrodes are essential for optimizing the performance of supercapacitors and other electrochemical devices.

Lastly, the thickness of the electrode material influences the ion diffusion distance and the internal resistance of the supercapacitor. A thinner electrode generally facilitates faster ion movement, improving the charge/discharge efficiency, whereas thicker electrodes may increase internal resistance and reduce performance [51].

3.15 Advantages and Limitations of Supercapacitors

Supercapacitors offer several key advantages compared to other energy storage systems (ESS). These benefits, particularly when contrasted with batteries, make supercapacitors an attractive alternative for various modern applications.

Firstly, Supercapacitors possess significantly higher power density than batteries. This means they can store and discharge large amounts of energy rapidly. For instance, while a supercapacitor can provide the necessary power to accelerate a vehicle quickly, a battery would take considerably longer to supply the same power [52]. In addition to having a higher power density than batteries, supercapacitors charge and discharge much faster. Typically, they can be fully charged within seconds or minutes, whereas batteries often require hours [53]. This feature makes supercapacitors ideal for applications demanding frequent charge/discharge cycles [54].

Furthermore, supercapacitors exhibit a substantially longer cycle life compared to batteries. While batteries tend to degrade after a few thousand cycles, supercapacitors can endure millions of charge/discharge cycles without significant performance loss. This translates to reduced maintenance and extended service life [55]. Supercapacitors also have greater energy efficiency than batteries, allowing a larger proportion of stored energy to be utilized. This makes them more ideal for energy-efficient applications [55].

Lastly, supercapacitors can function across a broader range of temperatures than batteries. This capability ensures reliable performance even under extreme temperature conditions. Moreover, supercapacitors are more environmentally friendly than batteries. They do not contain harmful heavy metals and are easier to recycle [55].

Supercapacitors, despite their advantages, have several limitations when compared to batteries. One of the primary drawbacks is their high manufacturing cost. The

production of supercapacitors involves materials and processes that are more expensive than those used in batteries, making them less economical for large-scale energy storage applications. This higher cost can be a significant barrier to their widespread adoption in sectors where cost-efficiency is critical [56].

Another limitation is the significant self-discharge characteristic of supercapacitors. Over time, they lose stored charge, which reduces their effectiveness for long-term energy storage. This self-discharge is more pronounced in supercapacitors than in batteries, making them less suitable for applications where energy needs to be stored for extended periods without frequent recharging. This issue limits their use in scenarios where energy retention over time is crucial, such as in backup power systems or long-duration energy storage [57].

Supercapacitors also suffer from lower energy density compared to batteries. This means that, for the same weight, a battery can store significantly more energy than a supercapacitor. As a result, supercapacitors are not suitable for applications requiring high-energy storage in a compact form. While supercapacitors excel in power density, enabling rapid energy release, their energy density remains a limiting factor for applications that require prolonged energy supply, such as portable electronic devices or electric vehicles [58].

Additionally, supercapacitors exhibit a linear discharge voltage during operation. Unlike batteries, which maintain a relatively stable voltage during discharge, the voltage of a supercapacitor decreases linearly as it discharges. This characteristic can pose challenges in applications that require a constant voltage, such as in devices powered by batteries that need steady energy output. For example, certain electronic devices or power systems that rely on stable voltage may find the linear voltage drop of supercapacitors less suitable [59].

The primary drawback of supercapacitors in comparison to batteries lies in their lower energy density. While batteries can store large amounts of energy but release it slowly, supercapacitors have a high power density, allowing them to deliver rapid bursts of energy. This distinction makes batteries more appropriate for applications requiring long-term, steady energy supply, such as powering electronic devices, while supercapacitors are ideal for applications that demand quick energy bursts, such as regenerative braking in vehicles or power smoothing in electrical grids [60].

3.16 Applications in Modern Technology

Supercapacitors have emerged as versatile energy storage solutions with applications across various sectors. One of their primary uses is storing energy generated from renewable sources such as solar and wind power. Given the intermittent nature of these energy sources, supercapacitors enable more reliable and efficient utilization by storing excess energy for later use. This capability is particularly important for enhancing the dependability of renewable energy systems [61].

Supercapacitors play a critical role in hybrid vehicles in the automotive industry by capturing energy during braking and providing additional power during acceleration. This improves fuel efficiency and contributes to reducing emissions, making hybrid vehicles more sustainable. Electric vehicles also use supercapacitors to improve overall performance and extend battery life [62].

Similarly, supercapacitors are increasingly used in portable electronic devices, including smartphones, laptops, and tablets. Their ability to charge and discharge rapidly allows these devices to charge faster and operate for extended periods, enhancing user convenience. This feature is particularly valuable in consumer electronics where quick charging times are a priority [63].

Supercapacitors are essential in industrial applications requiring rapid energy release. Electric vehicles (EVs) are used in regenerative braking systems, capturing energy during braking and quickly releasing it to assist in acceleration, improving energy efficiency. In industrial machinery such as forklifts and cranes, supercapacitors provide quick bursts of energy for heavy lifting and acceleration. Their high-power density ensures efficient operation in environments with frequent charge/discharge cycles. Supercapacitors also help stabilize electric grids by releasing energy rapidly during peak demand periods [64].

The military sector also benefits from supercapacitors' unique properties, employing them in applications like radars, military vehicles, and communication systems. Their robustness and capacity to perform under harsh conditions make them indispensable for critical uses [65].

3.17 Biomass: A Source for Carbon Materials

Biomass, a renewable resource derived from plants, trees, algae, crops, and organic waste, presents a compelling source for carbon materials. This organic material,

produced through photosynthesis, stores chemical energy that can be harnessed through various conversion processes [66]. The composition of biomass is diverse, including polysaccharides like cellulose and hemicellulose, and lignin, alongside elements such as carbon, oxygen, hydrogen, nitrogen, calcium, potassium, silicon, magnesium, aluminum, sulfur, iron, phosphorus, chlorine, sodium, manganese, and titanium. This composition varies depending on the source, with woody biomass generally having less ash and more carbon compared to agricultural biomass [67].

The conversion of biomass into valuable carbon materials involves thermal processes like pyrolysis, torrefaction, and gasification [68]. Pyrolysis, a thermal decomposition process, produces biochar, oils, and gases, with product distribution influenced by temperature, heating rate, and pressure [69]. Lower temperatures favor charcoal production, while higher temperatures increase gas yields. Torrefaction, a mild pyrolysis at 200-300°C, improves biomass properties by reducing moisture and increasing energy density [6]. Gasification converts biomass into a gaseous fuel, often for electricity generation [70]. These thermal processes are central to unlocking the potential of biomass for carbon material production.

Biomass-derived carbon materials, especially activated carbons, are finding increasing applications in energy storage devices such as supercapacitors and batteries. These materials benefit from their high surface area and porosity, which are critical for electrochemical performance [71**]**. These properties enhance ion storage and transport, making them efficient electrode materials. The electrochemical performance of these electrodes is related to their physical and chemical properties such as porosity, chemical composition, and surface functionalities [72].

The use of biomass as a carbon source offers several advantages: it is renewable and sustainable, decreasing our reliance on fossil fuels [73]. Moreover, it transforms waste into valuable products, contributing to the economy [74]. Sustainable biomass conversion can also contribute to reduced greenhouse gas emissions. However, there are challenges to address, such as understanding the relationships between biomass composition, processing conditions, and the performance of the derived carbon materials [75]. Further research is needed to optimize these materials for specific applications and to fully realize their potential.

3.18 Processing Biomass for Supercapacitor Applications

Biomass, a renewable resource, is increasingly used to produce carbon materials for supercapacitor electrodes [76]. The process involves several steps, from selecting the appropriate biomass to applying specific thermal and chemical treatments to achieve desired material properties [72]. The specific type of biomass influences the chemical composition and the resulting carbon material properties [72]. Cellulose, hemicellulose, and lignin are the primary components of biomass, and their proportions affect the carbon material's characteristics [77]. For example, lignin-rich biomass can be used to create porous carbon structures suitable for supercapacitor electrodes [78].

Pre-treatment methods can include washing, drying, and grinding [79]. These steps are important for removing impurities and ensuring uniform particle size before further processing. Biomass can undergo several thermal conversion processes, each with distinct characteristics and products. Combustion, torrefaction, liquefaction, steam explosion and hydrothermal carbonization (HTC) can be counted as the thermal conversion processes of biomass, which already mentioned briefly in introduction section of this thesis. Carbonization is frequently used to create activated carbon (AC), a porous carbon substance that has several uses, including the adsorption of both organic and inorganic substances. AC can be created through chemical or physical activation techniques [11]. Carbonization and high-temperature pyrolysis, usually at 800–1000 °C, with gases like steam or CO_2 present are both components of physical activation [72]. Chemical activation involves pyrolysis at a lower temperature, typically around 500 °C, after the use of chemical agents like $ZnCl_2$, H_3PO_4 or KOH. Because it requires less energy, chemical activation is frequently preferred. The use of H_3PO_4 in chemical activation of woody biomass has shown good results, due to its promotion of dehydration, depolymerization, and the formation of cross-linked structures. KOH activation involves the use of a nucleophilic OH group, leading to solubilization and fragmentation of the biomass and the formation of porous carbon materials [11].

The properties of biochar, including surface area and porosity, can be modified by process parameters such as temperature, heating rate, and residence time. Increasing the pyrolysis temperature generally results in a decrease in oxygen content and an increase in surface area [72].

3.19 Material Characteristics and Performance Metrics of Biomass

The physical and chemical properties of biomass-derived carbon materials, such as porosity, surface area, and chemical composition, significantly influence their electrochemical performance in supercapacitors [72].

High surface area provides more sites for charge accumulation, improving capacitance. Pore size distribution is also critical. Micropores (less than 2 nm) and mesopores (2-50 nm) facilitate ion transport and storage. The presence of heteroatoms like nitrogen, sulfur and oxygen can enhance the wettability and conductivity of the carbon material, and improve the capacitive performance [54].

Supercapacitor performance is evaluated using metrics such as specific capacitance, energy density, power density, and cycle life. Specific capacitance indicates the amount of charge a material can store per unit mass. Energy density represents the amount of energy stored in a supercapacitor. Power density indicates how fast the energy can be delivered. Cycle life is the number of charge-discharge cycles a supercapacitor can withstand without significant performance degradation [81].

4. MATERIAL & METHOD

4.1 Sample Preparation

All of the biomasses were grinded until their grain sizes are smaller than 250 micrometers. Custom design grinding machine in Fuel Technology Laboratory that can be seen in Figure 4.1 is used.

Figure 4.1 : Grinding machine.

4.2 Carbonization

Biomasses were carbonized using a tube furnace, as shown in Figure 4.2. All biomasses are carbonized at 900 ºC without any waiting time at the final temperatures. Nitrogen is used for carbonization. After putting the weighted biomass samples in a quartz boats, it is placed in the middle of the tube furnace. Both sides of the furnace are sealed with using Teflon and aluminum bands to prevent nitrogen leaking. At the righten side, nitrogen levels are measured. Left side, the pipe is put into small amount of water to observe nitrogen is passing through the furnace without leaking. It is understood by seeing bubbles in the water. After half an hour of nitrogen feeding, the

furnace started to carbonize the sample to the desired temperature and heating rate. The heating rate is chosen as 10 ºC. When it reaches its target temperature, it starts to cool down. Finally, when it is cooled to room temperature, the sample is taken out, weighted again to calculate efficiency, and used for further adsorption studies. Carbonized biomass is shown in Figure 4.3.

Figure 4.2: Tube furnace.

Figure 4.3 : Carbonized biomass.

4.3 Activation & Washing

After carbonization, samples are activated with solid KOH to enlarge their pore sizes. Each biomass is activated with 1:2, 1:3 and 1:4 ratios by mass, as can be seen on the Table 4.1 below.

Table 4.1 : Masses according to ratios.

Ratio	Sample (g)	KOH (g)
1:2	4	8
1:3	3	9
1:4	2,4	9,6

Samples and the related amount of KOH are mixed until a homogenous mixture is obtained. Then, the mixtures are put into the tube furnace at 800 °C with a heating rate of 10 °C per minute again.

After carbonized samples are activated, samples are washed with 100 mL HCl and 100 mL purified water solution to remove the impurities from activated samples. HCl solution is diluted with distilled water using graduated cylinder. After washing with HCl solution, samples are washed with 2 bottles of distilled water. All washing processes are made using a funnel, filter & filtering flask connected to a compressor for better & quicker washing. Washed samples are left to dry in an oven for a day at 60 °C to dry in a watch glass.

4.4 Solution Preparation

Each biomass is weighted 0.08 grams and mixed with 0.01 PVP and 3 mL of distilled water. Then, 0.3 gram of 10% PVP solution is put into the mixture using micropipette. After mixing for a day, the liquid mixture is used to coat coin cells. Coated coin cells are dried in oven at 60°C for 1 hour and used for measurements.

4.5 Extracted Sample Analysis

10 grams of ground sample (particle size below 250 μm) is mixed with 90 mL C_2H_5OH and 180 mL Benzene (1:2 v/v 270 mL). The solution is put into a cartridge and weighted, and extracted for 4 hours. Then, the sample is washed with alcohol to purify it from benzene. Then, C_2H_5OH is added and extracted again until the alcohol becomes colorless. After drying the sample with air, it is washed with 1 L boiling water for an

hour and washed again with 500 mL boiling distilled water. Finally, it dried again with air and weighed. Process flow can be seen in Figure 4.4.

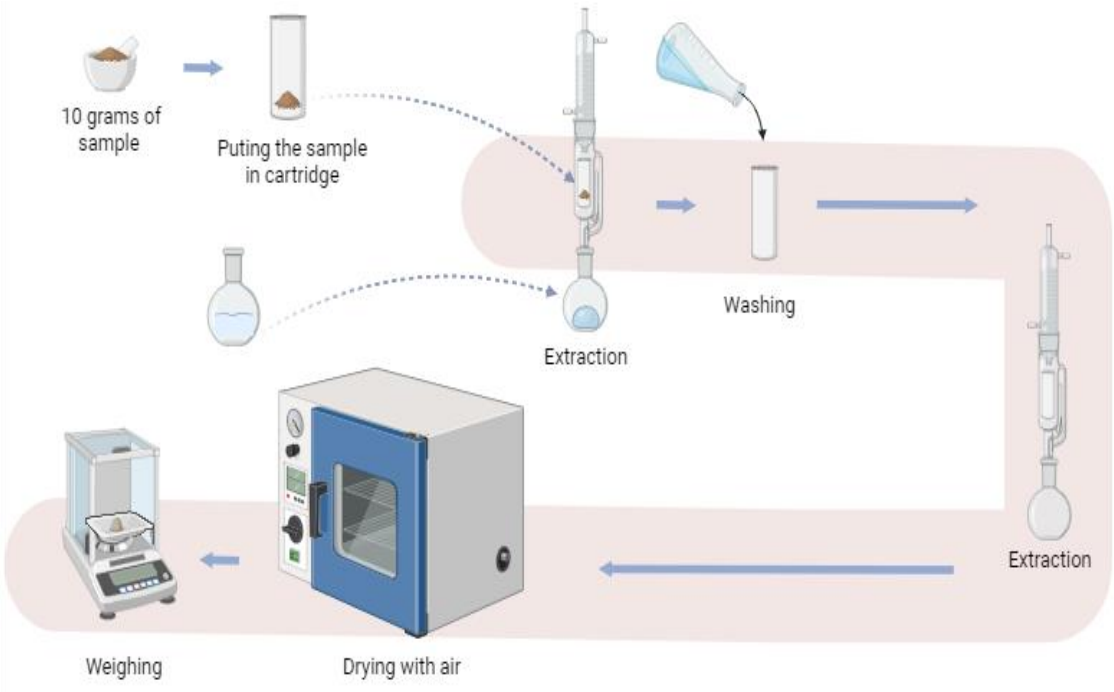

Figure 4.4 : Extracted sample analysis workflow.

4.6 Hollocellulose Analysis

2-5 grams of extracted sample is mixed with 100 mL distilled water, 1,5 grams $NaClO_2$, and 5 mL 10% CH_3COOH. Heated in a water bath for 30 minutes at 70 °C, and 5 mL 10% CH_3COOH is added. Heated in a water bath for an hour at 70 °C again, and 1,5 gram $NaClO_2$ is added. Then, continue to add $NaClO_2$ until hollocellulose becomes colorless. The sample is cooled in icy water, filtered, and washed with cold water and acetone. Finally, it is dried and weighed. Process flow can be seen in Figure 4.5.

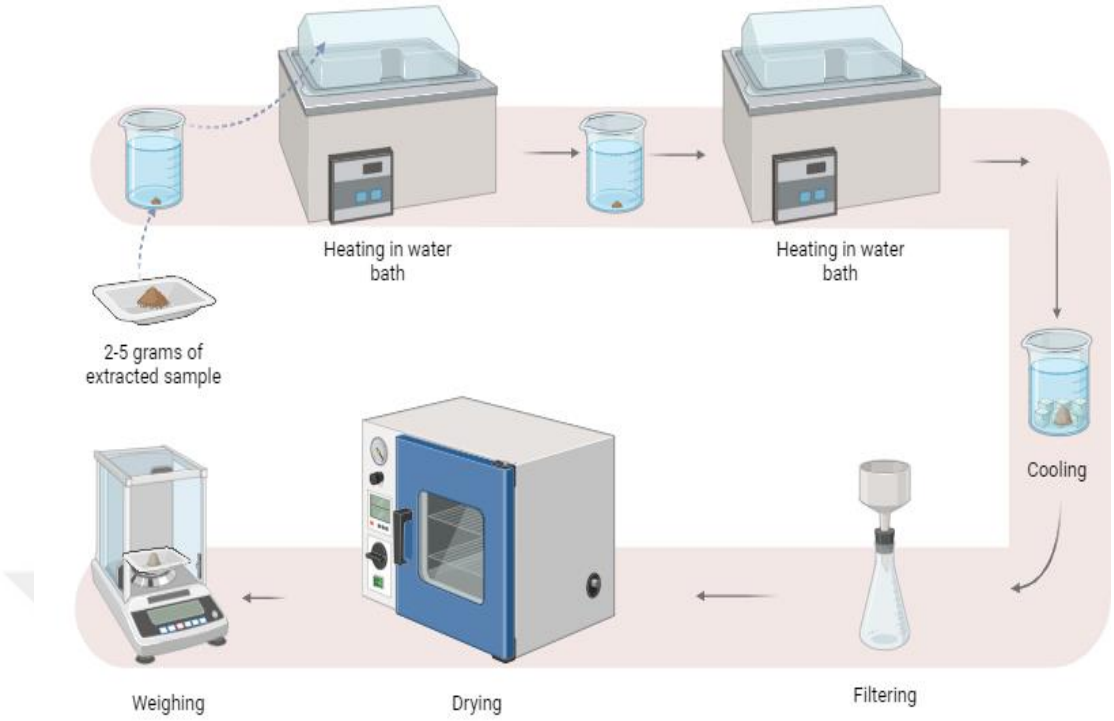

Figure 4.5 : Hollocellulose analysis workflow.

4.7 Lignin Analysis

1 gram of extracted sample is prepared. 665 mL H_2SO_4 and 300 mL distilled water is added (until having a 1L 72% solution) and cooled. 50 mL 72% H_2SO_4 is mixed with 1 gram of sample in a 300 mL flask. Then, it is mixed with a glass baguette and waited at room temperature for 2 hours. The cartridge is weighted at this step, and the sample is filtered with 500 mL of boiling water. Then, it is dried at 105 °C for 2 hours and weighed again. After burning at 600°C, the weight difference is calculated as the lignin content. Process flow can be seen in Figure 4.6.

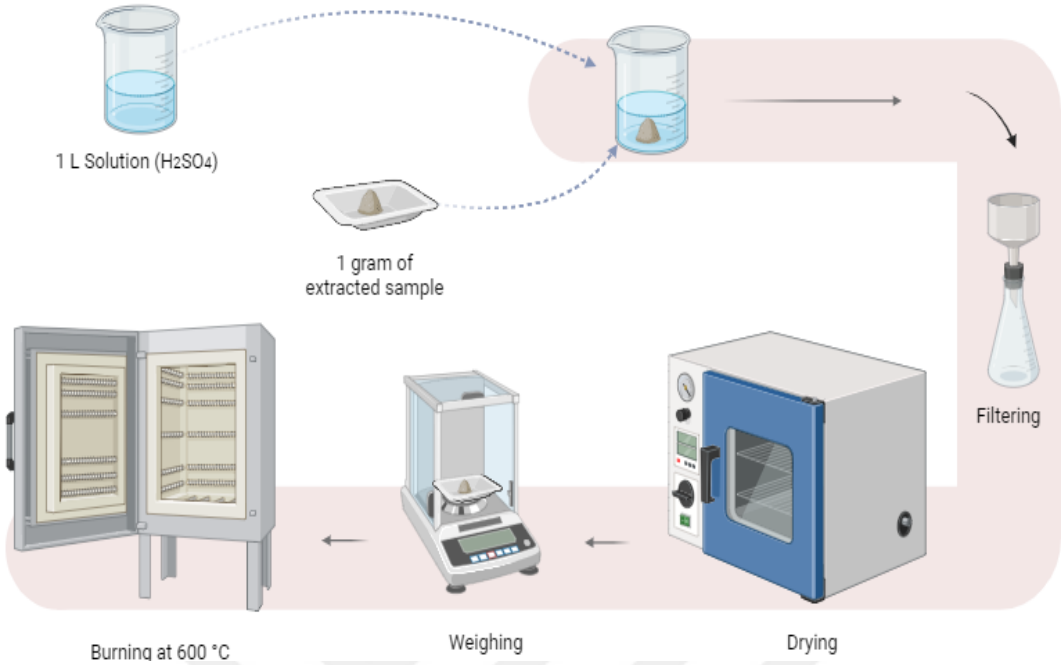

Figure 4.6 : Lignin analysis workflow.

4.8 Structural Characterization & Electrochemical Measurements

For structural characterization of samples; Fourier Transform Infrared (FTIR), Raman spectroscopy, X-ray diffraction (XRD), and Brunauer–Emmett–Teller (BET) measurements are conducted in ITU Chemical Engineering laboratories. Cyclic Voltammetry (CV), Galvanostatic Charge - Discharge (GCD), Impedance (EIS) and Retention analysis are made to analyse electrochemical performances of samples. 3D printed custom-made mechanism and Corrtest device which can be seen in Figure 4.7 is used for measurements.

Figure 4.7 : Corrtest device.

5. RESULTS & DISCUSSION

5.1 FTIR Analysis

The analysis of infrared spectra reveals the molecular composition and concentrations within a sample. Figure 5.1 shows that not activated biomass (DL) showed significant absorption band at nearly 1290 cm^{-1}, which indicates lignocellulosic biomass naturally has oxygenetad functional groups in its structure, including -OH groups from cellulose and hemicellulose and C=O groups from lignin as indicated in Table 5.1 [82].

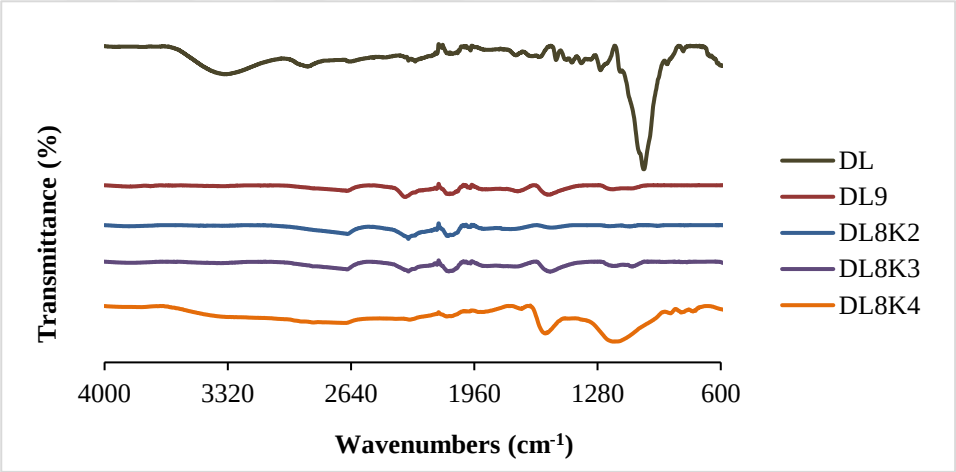

Figure 5.1 : FTIR spectra.

Table 5.1 : Chemical bond types according to peaks [83].

Peak (cm^{-1})	Bond	Related Structure
3300	O-H	Moisture, cellulose/hemicellulose
2900	C-H	Cellulose, Hemicellulose, Lignin
1720	C=O	Hemicellulose
1590	C=C	Lignin
1020	C-O-C	Cellulose, Lignin

Upon thermal treatment at 900 °C, the spectrum of DL9 shows a significant flattening, with the disappearance or attenuation of several prominent bands. This indicates the decomposition and volatilization of labile oxygen-containing groups, consistent with the known effects of high-temperature carbonization and pyrolysis [84]. The reduction in hydroxyl and carbonyl peaks reflects the conversion of the biomass to a more carbon-rich, aromatic structure.

In the case of chemically activated samples (DL8K2, DL8K3, and DL8K4), which are activated with KOH and carbonized at 800 °C, the FTIR spectra show some reappearance or persistence of certain bands compared to DL9, particularly in the 1000–1200 cm^{-1} and 1400–1600 cm^{-1} regions. These are typically associated with C–O stretching (alcohols, phenols, esters) and C=C aromatic skeletal vibrations. Among these, DL8K4, which is the sample with the highest KOH ratio, displays the most pronounced absorption features, suggesting that increased KOH dosage may enhance surface oxidation and/or introduce new functional groups.

This behavior is consistent with literature reports that KOH activation not only increases the surface area and porosity but also introduces oxygenated surface functionalities, such as hydroxyls, carbonyls, and carboxylic groups, depending on the activation parameters [85]. The chemical reactions between KOH and the carbon matrix can generate microporosity and functional groups via redox and gas-evolving reactions, leaving behind surface oxygen species that FTIR can detect.

Structural analysis results shown at Table 5.2 also supported FTIR results, that each biomass has large percent of holocellulose in their content.

Table 5.2 : Structural analysis results.

Content	Cedar	Scots Pine	Eastern Spruce
Holocellulose	61.73%	62.24%	71.84%
Lignin	21.02%	29.48%	19.40%
Extractives	17.25%	8.27%	8.49%

5.2 Raman Spectroscopy Results

Raman spectroscopy has long been central to the study and characterization of graphitic materials, being widely applied in the last four decades the study of a variety of materials such as pyrolytic graphite, carbon fibers, glassy carbon, pitch-based graphitic foams, nano graphite ribbons, fullerenes, carbon nanotubes, and graphene.

The peak at 1580 $cm^{-1,}$ named D band, is associated with Raman scattering of C-C bonds being broken, hence indicating graphite existence. The other peak at 1350 cm^{-1} is related with graphitic structures or carbonyl groups [86]. As showed in Figure 5.2 DL9, DL8K2, DL8K3 and DL8K4 results showed G-band at ~1300 and D-band at 1600 cm^{-1} , which is compatible with crystalline graphene's Raman spectra [87].

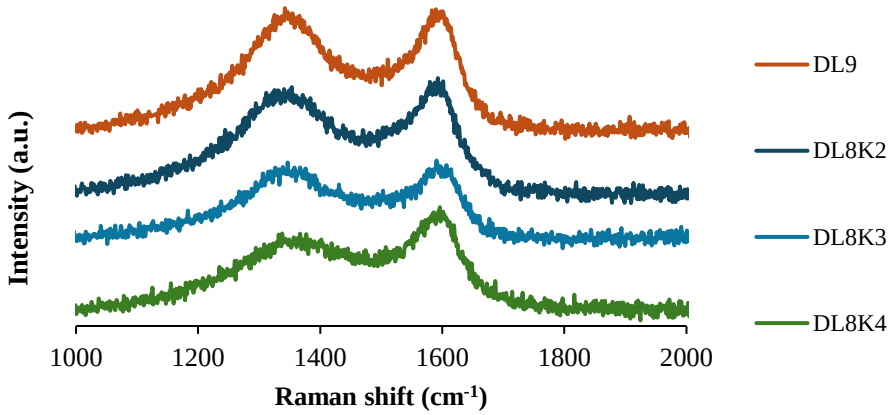

Figure 5.2: Raman spectra.

5.3 X-ray Diffraction (XRD) Results

XRD technique is the method most commonly used for quantitative analysis. This method is used determine the structural parameters (such as interplanar distance and crystallite size) of carbon materials directly from their X-ray diffraction patterns, which mainly define their structure [87]. Figure 5.3 presents that all samples exhibit peaks around 23° and 43°, which correspond to the (002) and (100) planes of turbostratic or amorphous carbon. DL9 shows broadest 002 peak, meaning less organized graphitic structure compared to thermally activated samples. DL8K2 and DL8K4 have slightly sharper 002 peaks than DL9 while the sharpest 002 and 100

peaks are observed with DL8K3. DL8K3 results also align with BET results, indicating that the 1:3 w/w activation ratio creates micropores and carbon molecules become more organized.

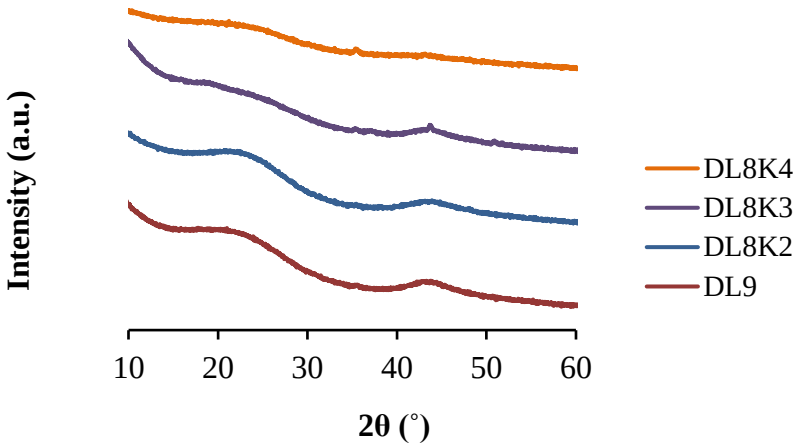

Figure 5.3: XRD Spectra.

5.4 Brunauer-Emmett-Teller (BET) Analysis

The Brunauer-Emmett-Teller (BET) method has been used extensively to characterize the surface areas of porous materials by semi-empirical fitting of gas-adsorption isotherms [88]. Table 3 shows BET results of Eastern Spruce samples. According to results, activating samples with KOH and increasing the KOH ratio resulted in enlarging the BET surface area (S_{BET}), micropore surface area (S_{mic}), micropore volume (V_{mic}) and total pore volume (V_{tot}). However, DL8K4 sample had smaller BET surface area than DL8K3, this observation can be explained by either pores collapsing or agglomeration. Micropore surface area, micropore volume and total pore volume also showed decrease between DL8K3 and DL8K4, this may be evidence that macropores are not affected by activation ratio as micropores. Furthermore, average pore volume (Dp,ave) decreased after activation but not changed significantly with KOH ratio.

Table 5.3: BET results of Eastern Spruce samples.

	DL9	DL8K2	DL8K3	DL8K4
S_{BET} (m^2/g)	226,62	803,56	1294,97	555,84
S_{mic} (m^2/g)	186,78	773,82	1213,09	520,35
V_{mic} (cm^3/g)	0,07	0,30	0,48	0,21
V_{tot} (cm^3/g)	0,11	0,33	0,56	0,26
V_{mic}/V_{tot} (%)	67,62	91,66	87,03	80,21
$D_{p,ave}$ (nm)	1,95	1,62	1,72	1,84

For further analysis, Nitrogen adsorption/ desorption isotherm of DL8K4 is also plotted. Figure 5.4 shows hierarchical porous carbon structure, as sudden decrease in absorved volume is observed with lower relative pressure ratios indicate micropores and sudden increase in absorved volume with higher relative pressure ratio indicate macropore presence [89].

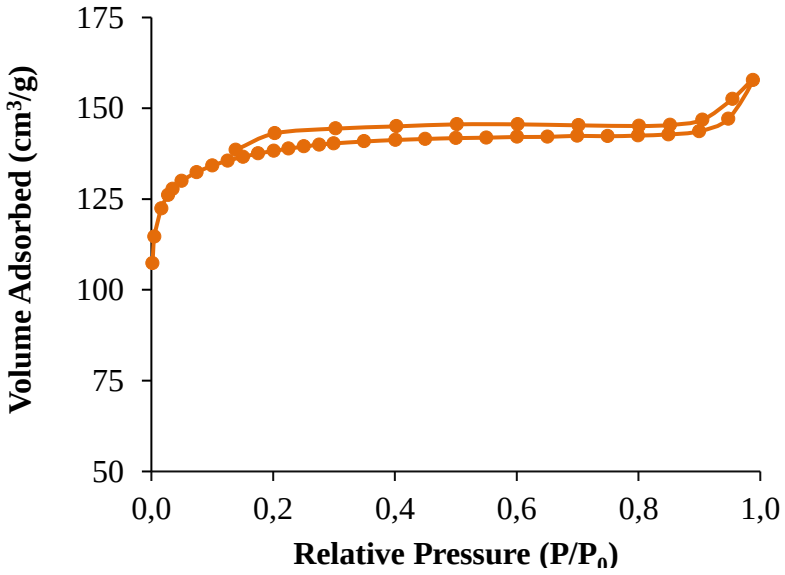

Figure 5.4 : Nitrogen adsorption/ desorption isotherm.

5.5 Cyclic Voltammetry (CV) Analysis Results

Cyclic Voltammetry method is commonly used in understanding electrochemical character of samples. The cyclic waves are called coltammograms and electric potential at the electrode surface varies with time during triangular spans. This voltammograms gives insights about electrolyte's reactivity and mass transport properties. The curve shows the relation between rates of electrolysis and the transport of reactants to the electrode surface by diffusion. The current rate is changed during measurements and when calculating the capacitance of supercapacitor, ionic concentration and area is taken into account [90].

In this study, the CV curves of all samples are recorded over potential of -1.0 V to 0 V and different current densities: 10, 25, 50, 100, 150, 200, 250, 300 and 500 mV/s. As shown in Figure 5.5, 5.6, 5.7 and 5.8 DL8K3 showed the most rectangular and symmetric CV profile, especially at lower scan rates. DL8K4 also has a promising CV profile but the profile is slightly more distorted compared to DL8K3, this finding may be resulted from either pore blockage or overly aggressive activation [90]. Narrower curves are obtained with DL8K2 sample, indicating lower capatince and ion transport which also correlated with its lower BET surface area (226.62 m^2/g). Not activated sample DL9 has the least capacitive behavior and non-ideal CV profile, consistent with its non-activated structure.

With all samples, best performance is observed at 500 mV/s scan rate, leading to conclusion that increasing scan rate enhances supercapacitor efficiency. 500 mV/s performance of the samples are compared in Figure 5.9, clearly showing that DL8K3 has the largest surface area than other samples. The superior CV performance of DL8K3 is directly correlated with its highest BET surface area (1294,97 m2/g), microporosity (87%) and relatively enhanced graphitic disordering (sharper XRD (002)/(100) peaks).

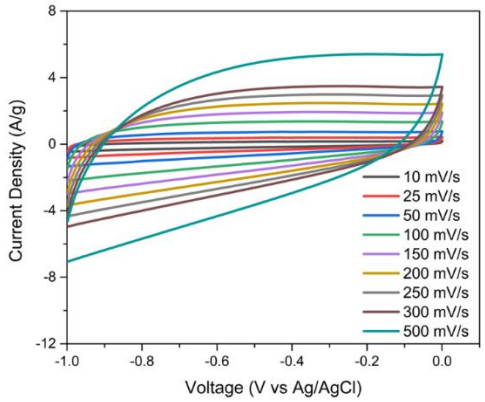

Figure 5.5 : CV plot of DL9.

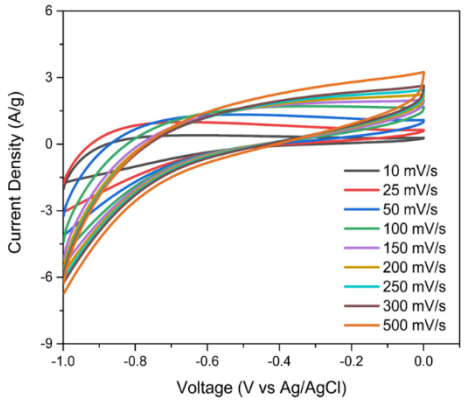

Figure 5.6: CV plot of DL8K2.

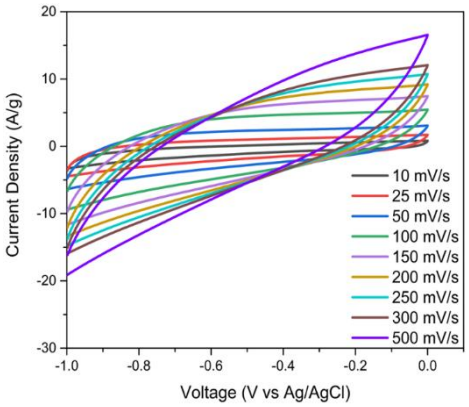

Figure 5.7: CV plot of DL8K3.

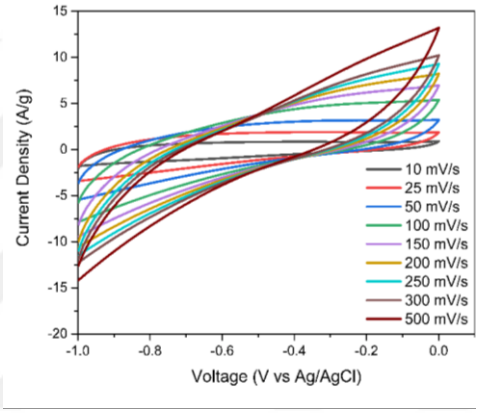

Figure 5.8 : CV plot of DL8K4.

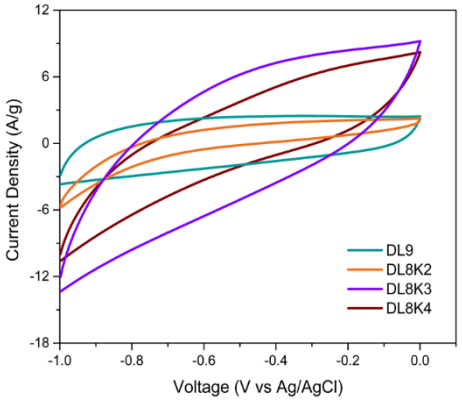

Figure 5.9: CV plot comparison

5.6 Galvanostatic Charge-Discharge (GCD) Analysis Results

Galvanostatic Charge-Discharge (GCD) analysis is conducted to assess the performance of energy storage systems like capacitors. GCD analysis is applied to a material by giving it positive and negative currents and charging and discharging it within a specified potential limit. Repeating multiple cycles gives GCD profiles of samples, which are used to evaluate the quality of capacitive behavior [91]. The charge and discharge curves are symmetrical and this indicates high reversibility [92].

Eastern spruce samples are underwent GCD analysis with currents of 0.1, 0.5, 1, 1.5 and 2 A/g. Figure 5.10, 5.11, 5.12 and 5.13 shows GCD profiles of DL9, DL8K2, DL8K3 and DL8K4 respectively. X-axis indicates the time needed to charge and discharge each sample. Charging capacity is dependent on current as can be seen in all figures. As applied current increased, the time required to charge & discharge each sample is decreased. All samples performed best under the current of 2 A/g, this conclusion also means all samples had their best capacititive ability with the highest current applied.

Figure 5.14 is the comparison of all samples under 0,1 A/g. As also can be seen in this figure, DL8K3 and DL8K4's GCD profiles showed the best performances while DL8K2 was significantly lower and DL9 showed the poorest charging profile – indicating higher internal resistance. This can be also supported with BET results, DL8K3 and DLK4 having much more BET surface area than the other samples back-up them having better performences despite DL8K4 having minor distortion observed in CV. Figure 5.15 shows GCD profile of DLK4 repeated with the cycle number of 1, 1000 and 2000. Mentioned GCD profile showed time need to charge & discharge slightly lowered when repeating GCD over 1000th and 2500th cycles, this can be explained by having significant residual voltage at the end of each GCD cycle, meaning that once an electrode is charged, when the second or subsequent GCD is performed system will require less time to charge [93].

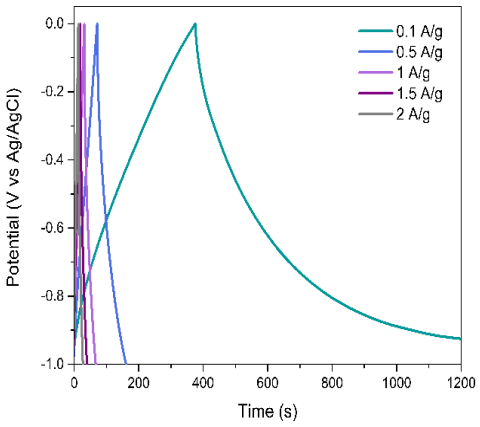

Figure 5.10 : GCD plot of DL9.

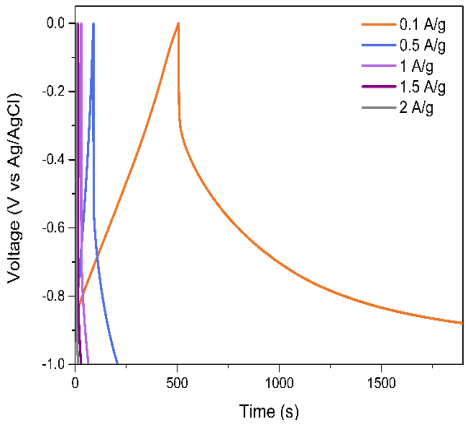

Figure 5.11 : GCD plot of DL8K2.

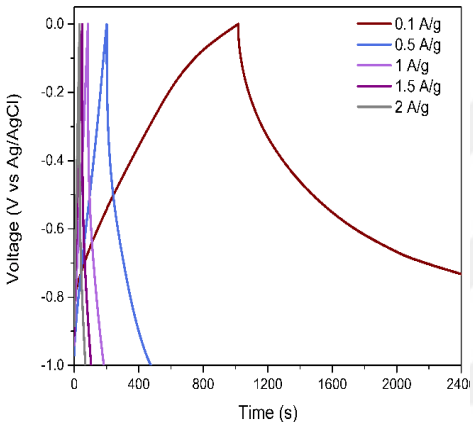

Figure 5.12 : GCD plot of DL8K3.

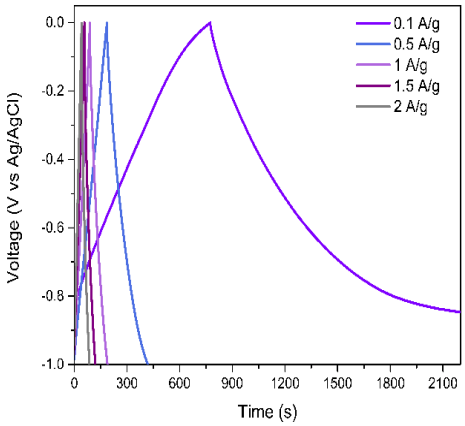

Figure 5.13 : GCD plot of DL8K4.

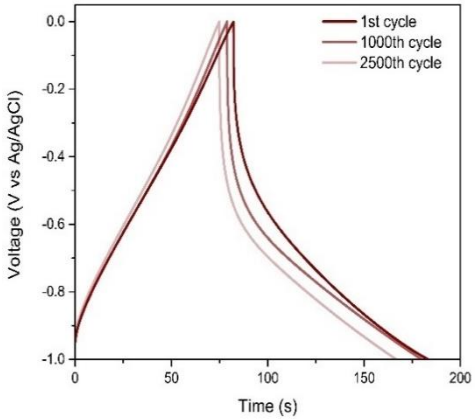

Figure 5.14 : Comparison of GCD's at 2 A/g

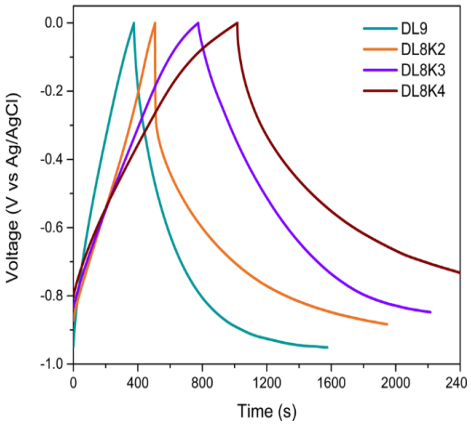

Figure 5.15 : Repeated GCD of DL8K4.

The retention plot is drawn to gain more insight of the long-term cyclic stability of DL8K4. Since GCD analysis is conducted until 2500th cycle, Capacitance Retention (%) is plotted against cycle number as can be seen in Figure 5.16. The DL8K4 coated electrode exhibits excellent stability with a capacitance retention of over 90% after 2500 cycles, aligning with the performance benchmarks described in previous studies on high-performance carbon-based supercapacitors.

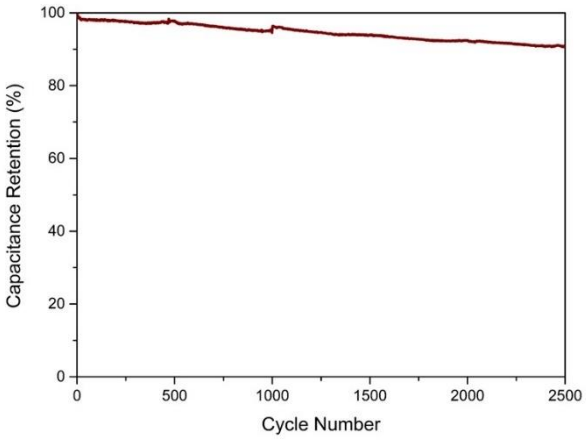

Figure 5.16 : Retention Analysis of DL8K4.

5.7 Electrochemical Impedance Spectroscopy (EIS) Nyquist plot

Nyquist plots are used to analyse internal resistance of samples. X-axis indicates the impedance, and higher internal resistance is observed by a shift to the right. [94]. Figure 5.17 shows Nyquist plot of each sample and it is seen that DL8K4 has the lowest resistance since the line intercepts with x axis in lower values, suggesting better ionic conductivity/electrolyte access. DL9 has the highest resistance - likely due to the lack of chemical activation. In the low-frequency region, DL8K3 has more vertical line compared to others. This plot suggests that DL8K3 has faster ion diffusion and more efficient charge storage while it has similar internal resistance with DL8K4.

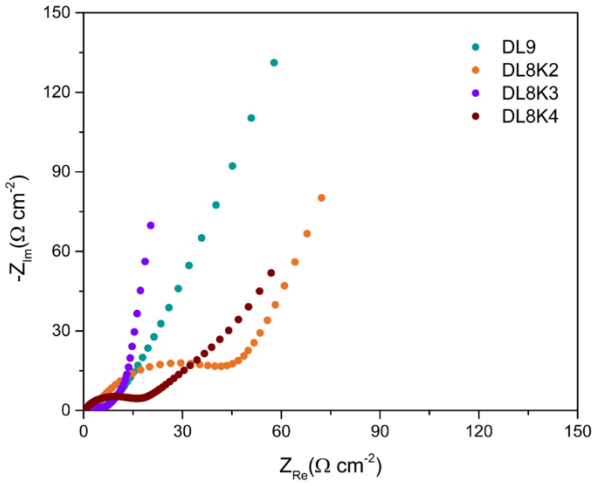

Figure 5.17 : Nyquist plot of samples.

5.8 Capacitance Calculations

Capacitance calculations are made using following formula:

$$C_a = \frac{I\Delta t}{A\Delta V} \tag{5.1}$$

Where I stands for discharge current (mA), ΔV standsds for voltage difference (V), Δt stands for the time required for the voltage difference (s) and A indicates the active area (cm^2).

When calculating capacitance, active area is an area of a circle with 0.9 cm diameter. All calculations were made between -0.8 and 0.3 V, hence ΔV is 1.1 V.

Δt is the time between the last observed peak on the GCD graph and the last point of measurement.

I is observed on GCD graphs as 0,1, 0,5, 1, 1,5 and 2 A/g. While calculating capacitance, I as multiplied by the corresponding sample weight and I unit is converted to miliampere.

Specific capacitance results of samples are shown in Figure 5.18. Poorest specific capacitance is observed at DL9 and DLK3 and DL8K4 showed similar lines. As current density increased, specific capasitance decreased in all samples – which can be explained by polarization resistance increasing with the amount of charge that are being transferred [89].

.

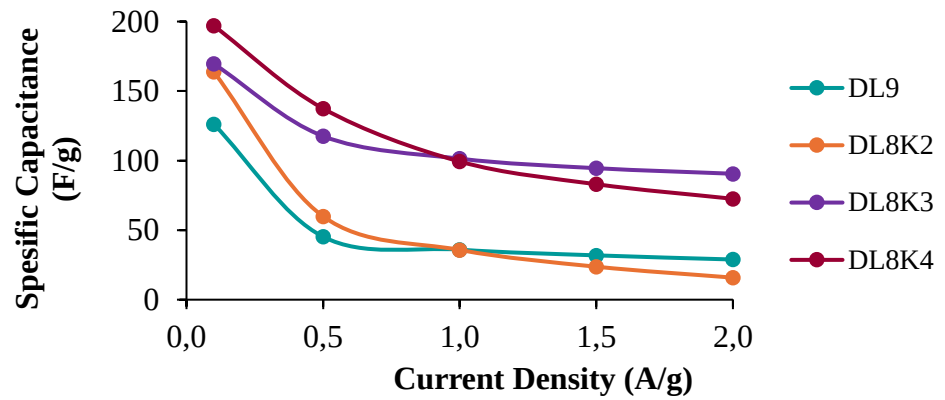

Figure 5.18 : Specific capacitance of samples with increased current densities.

Using formula (1), calculations are made and highest specific capacitance is observed in DL8K4 sample with 0,1 A/g current density. All capacitance values are listed in Table 5.4 for specified current densities.

Table 5.4 : Capacitance Calculations.

	Specific Capacitance (F/g)			
Current Density (A/g)	DL9	DL8K2	DL8K3	DL8K4
0,1	126	164	170	197
0,5	45	60	118	137
1	36	36	101	99
1,5	32	24	95	83
2	29	16	91	73

DL8K4 sample is taken into consideration while plotting Ragone, since highest specific capacitance is oberved with this sample. Figure 5.19 is called Ragone plot, showing power over energy density, which is the most important parameter for energy storage systems [95]. As can be seen in the figure, as power density increases, energy density tend to decrease. The trade-off means faster charge/discharge limits the total energy storage due to reduced time for ion adsorption. From the plot, it is observed that DL8K4 delivers an energy density of nearly 30 Wh/kg at nearly 100 W/kg. This performance suggests that pore architecture and high surface area supports ion diffusion, moderate graphitic structure as seen in XRD results align with electrical conductivity and chemical stability as confirmed in retention test make DL8K4 a promising supercapacitor coating material.

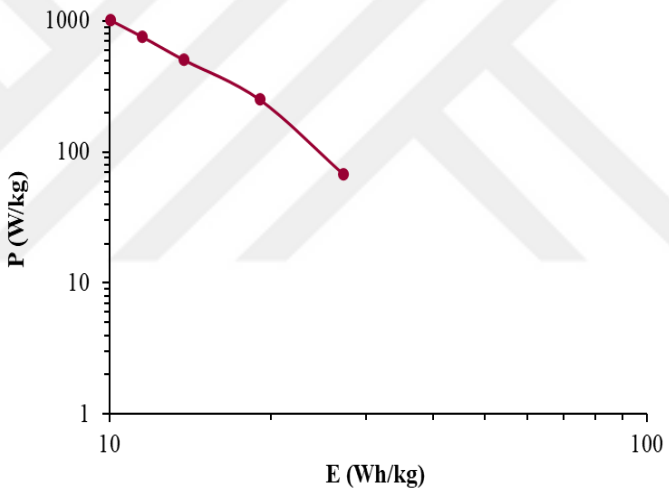

Figure 5.19 : Ragone Plot of DL8K4.

6. CONCLUSION

This study investigated forest biomass-derived carbon materials for their potential application as supercapacitor electrodes. One sample (DL9) was torrefied at 900 °C without activation, while three others (DL8K2, DL8K3, DL8K4) underwent chemical activation with KOH at 800 °C using varying weight ratios (1:2, 1:3, 1:4, respectively) after torrefaction at 900 °C. The influence of activation ratio on electrochemical properties was evaluated through BET surface area analysis, FTIR, Raman, XRD, cyclic voltammetry (CV), galvanostatic charge-discharge (GCD), electrochemical impedance spectroscopy (EIS), cycling stability, and Ragone plot analysis.

Among all samples, DL8K3, prepared at a 1:3 KOH-to-carbon ratio, exhibited the most favorable combination of properties: the highest surface area (1294.97 m^2/g), predominant microporosity (~87%), improved structural ordering (XRD), and the most ideal capacitive behavior (CV and GCD). It also showed excellent rate capability, low internal resistance (EIS), and competitive energy and power densities (Ragone plot), making it the most promising candidate for high-performance supercapacitor applications.

DL8K4, while slightly less porous, retained significant electrochemical performance and exhibited the best cycling stability, maintaining over 90% capacitance after 2500 cycles. In contrast, DL8K2 and DL9 showed inferior performance, likely due to underactivation and lack of developed porosity. Notably, a possible mislabeling between DL9 and DL8K2 was suggested based on BET and electrochemical data.

REFERENCES

[1] **Maamoun N, Kennedy R, Jin XM, Urpelainen J.** (2020). Identifying coal-fired power plants for early retirement. Renew Sustain Energy Rev 126:109833. Retrieved from https://doi.org/10. 1016/j. rser. 2020.109833.

[2] **Yang Y, Campana PE, Yan JY.** (2020). Potential of unsubsidized distributed solar PV to replace coal-fired power plants, and profits classification in Chinese cities. Renew Sustain Energy Rev 131:109967. Retrieved from https:// doi. org/ 10. 1016/j. rser. 2020. 109967.

[3] **Farghali M, Osman AI, Umetsu K, Rooney DW.** (2022). Integration of biogas systems into a carbon zero and hydrogen economy: a review. Environ Chem Lett. Retrieved from https:// doi. org/ 10. 1007/s10311- 022-01468-z.

[4] **Rahman A, Farrok O, Haque MM.** (2022). Environmental impact of renewable energy source based electrical power plants: Solar, wind, hydroelectric, biomass, geothermal, tidal, ocean, and osmotic. Renew Sustain Energy Rev 161:112279. Retrieved from https:// doi.org/ 10. 1016/j. rser. 2022. 112279.

[5] **McKendry, P.** (2002). Energy production from biomass (part 1): Overview of biomass. Bioresource Technology, 83(1). Retrieved from https://doi.org/10.1016/S0960-8524(01)00118-3.

[6] **Lewandowski, W. M., Ryms, M., & Kosakowski, W.** (2020). Thermal biomass conversion: A review. Processes, 8(5). Retrieved from https://doi.org/10.3390/PR8050516.

[7] **Libich, J., Máca, J., Vondrák, J., Čech, O., & Sedlaříková, M.** (2018). Supercapacitors: Properties and applications. Journal of Energy Storage, 17. Retrieved from https://doi.org/10.1016/j.est.2018.03.012.

[8] **Vijayakumar, M., Santhosh, R., Adduru, J., Rao, T. N., & Karthik, M.** (2018). Activated carbon fibres as high performance supercapacitor electrodes with commercial level mass loading. Carbon, 140. Retrieved from https://doi.org/10.1016/j.carbon.2018.08.052.

[9] **Berrueta, A., Ursua, A., Martin, I. S., Eftekhari, A., & Sanchis, P.** (2019). Supercapacitors: electrical characteristics, modeling, applications, and

future trends. *IEEE Access*, *7*, 50869–50896. Retrieved from https://doi.org/10.1109/access.2019.2908558.

[10] **Yuan, C., Xu, H., El-Khodary, S. A., Ni, G., Esakkimuthu, S., Zhong, S., & Wang, S**. (2024). Recent advances and challenges in biomass-derived carbon materials for supercapacitors: A review. *Fuel*, *362*, 130795. Retrieved from https://doi.org/10.1016/j.fuel.2023.130795.

[11] **Osman, A. I., Abdelkader, A., Farrell, C., Rooney, D., & Morgan, K.** (2019). Reusing, recycling and up-cycling of biomass: A review of practical and kinetic modelling approaches. *Fuel Processing Technology*, *192*, 179–202. Retrieved from https://doi.org/10.1016/j.fuproc.2019.04.026.

[12] **Osman, A. I., Abdelkader, A., Farrell, C., Rooney, D., & Morgan, K.** (2019b). Reusing, recycling and up-cycling of biomass: A review of practical and kinetic modelling approaches. *Fuel Processing Technology*, *192*, 179–202. Retrieved from https://doi.org/10.1016/j.fuproc.2019.04.026.

[13] **Tiwari, S. K., Bystrzejewski, M., De Adhikari, A., Huczko, A., & Wang, N.** (2022). Methods for the conversion of biomass waste into value-added carbon nanomaterials: Recent progress and applications. *Progress in Energy and Combustion Science*, *92*, 101023. Retrieved from https://doi.org/10.1016/j.pecs.2022.101023.

[14] **Meir, P., Shenkin, A., Disney, M., Rowland, L., Malhi, Y., Herold, M., & Da Costa, A. C. L.** (2017). Plant Structure-Function Relationships and Woody Tissue Respiration: Upscaling to Forests from Laser-Derived Measurements. In *Advances in photosynthesis and respiration* (pp. 89–105). Retrieved from https://doi.org/10.1007/978-3-319-68703-2_5.

[15] **Barnett, J. R., & Jeronimidis, G.** (2003). *Wood Quality and its Biological Basis* (Issue 1). Retrieved from http://ci.nii.ac.jp/ncid/BA66599741.

[16] **Burgert, I., & Keplinger, T.** (2013). Plant micro- and nanomechanics: experimental techniques for plant cell-wall analysis. *Journal of Experimental Botany*, *64*(15), 4635–4649. Retrieved from https://doi.org/10.1093/jxb/ert255.

[17] **Petráš, R., Mecko, J., Krupová, D., & Pažitný, A.** (2020). Aboveground biomass basic density of hardwoods tree species. *Wood Research*, *65*(6), 1001–1012. Retrieved from https://doi.org/10.37763/wr.1336-4561/65.6.10011012.

[18] **Crosby, R., Das, D., & Paul, M. C.** (2024). Numerical study and experimental validation of a porous biochar supported form stable composite for thermal energy storage. *Journal of Energy Storage*, *99*, 113314. Retrieved from https://doi.org/10.1016/j.est.2024.113314.

[19] **Liang, C., Bao, J., Li, C., Huang, H., Chen, C., Lou, Y., Lu, H., Lin, H., Shi, Z., & Feng, S.** (2017). One-dimensional hierarchically porous carbon from biomass with high capacitance as supercapacitor materials.

Microporous and Mesoporous Materials, *251*, 77–82. Retrieved from https://doi.org/10.1016/j.micromeso.2017.05.044.

[20] **Kober, T., Schiffer, H., Densing, M., & Panos, E.** (2020). Global energy perspectives to 2060 – WEC's World Energy Scenarios 2019. *Energy Strategy Reviews*, *31*, 100523. Retrieved from https://doi.org/10.1016/j.esr.2020.100523.

[21] **Jaiswal, K. K., Chowdhury, C. R., Yadav, D., Verma, R., Dutta, S., Jaiswal, K. S., SangmeshB, N., & Karuppasamy, K. S. K**. (2022). Renewable and sustainable clean energy development and impact on social, economic, and environmental health. *Energy Nexus*, *7*, 100118. Retrieved from https://doi.org/10.1016/j.nexus.2022.100118.

[22] **Mitali, J., Dhinakaran, S., & Mohamad, A.** (2022b). Energy storage systems: a review. *Energy Storage and Saving*, *1*(3), 166–216. Retrieved from https://doi.org/10.1016/j.enss.2022.07.002.

[23] **Stadler, I., & Sterner, M.** (2018). Urban energy storage and sector coupling. In *Elsevier eBooks* (pp. 225–244). Retrieved from https://doi.org/10.1016/b978-0-08-102074-6.00026-7.

[24] **Uner D.** Storage of Chemical Energy and Nuclear Materials, Energy storage systems- Volume II., UNESCO-EOLSS sample chapters. ⟨http://www.eolss.net/samplechapters/ c08/e3-14-05.pdf⟩ [07.10.2015].

[25] **Guney, M. S., & Tepe, Y.** (2016b). Classification and assessment of energy storage systems. *Renewable and Sustainable Energy Reviews*, *75*, 1187–1197. Retrieved from https://doi.org/10.1016/j.rser.2016.11.102.

[26] **Miller, M. A., Petrasch, J., Randhir, K., Rahmatian, N., & Klausner, J.** (2020). Chemical energy storage. In *Elsevier eBooks* (pp. 249–292). Retrieved from https://doi.org/10.1016/b978-0-12-819892-6.00005-8.

[27] **Sadeq, Abdellatif.** (2023) Energy Storage Systems: A Comprehensive Guide. 10.13980/RG.2.2.33942.55771.

[28] **Dincer, Ibrahim & Rosen, Marc.** (2010). Thermal energy storage (TES) methods. Thermal Energy Storage: Systems and Applications. 83-190.

[29] **Enescu, D., Chicco, G., Porumb, R., & Seritan, G.** (2020). Thermal energy storage for grid applications: Current status and emerging trends. *Energies*, *13*(2), 340. Retrieved from https://doi.org/10.3390/en13020340.

[30] **Chen H, Cong TN, Yang W, Tan C, Li Y, Ding Y.** Progress in electrical energy storage system: a critical review. Prog Nat Sci 2009;19:291–312.

[31] **Wagner L.** Overview of energy storage methods, http://www.moraassociates.com/publications/0712%20Energy%20storage.pdf; 2007.

[32] **Helmholtz H.** ``Studien über electrische Grenzschichten," *Ann. Phys.*, vol. 243, no. 7, pp. 337_382, 1879.

[33] **H. Wang and L. Pilon,** ``Accurate simulations of electric double layer capacitance of ultramicroelectrodes," *J. Phys. Chem. C*, vol. 115, no. 33, pp. 16711_16719, 2011.

[34] **A. J. Bard and L. R. Faulkner,** *Electrochemical Methods: Fundamentals and Applications*. Hoboken, NJ, USA: Wiley, 2001.

[35] **O. Stern,** ``*The theory of the electrolytic double_layer," Z. Elektrochem, vol. 30, no. 508, pp. 1014_1020, 1924.*

[36] **Moftah, Abdeladim.** *(2019). Review of Supercapacitor Technology.*

[37] **Meena, D., Kumar, R., Gupta, S., Khan, O., Gupta, D., & Singh, M.** (2023). Energy storage in the 21st century: A comprehensive review on factors enhancing the next-generation supercapacitor mechanisms. *Journal of Energy Storage*, *72*, 109323. Retrieved from https://doi.org/10.1016/j.est.2023.109323.

[38] **Amir, M., Deshmukh, R. G., Khalid, H. M., Said, Z., Raza, A., Muyeen, S., Nizami, A., Elavarasan, R. M., Saidur, R., & Sopian, K.** (2023). Energy storage technologies: An integrated survey of developments, global economical/environmental effects, optimal scheduling model, and sustainable adaption policies. *Journal of Energy Storage*, *72*, 108694. Retrieved from https://doi.org/10.1016/j.est.2023.108694.

[39] **Davies, A., & Yu, A.** (2011). Material advancements in supercapacitors: From activated carbon to carbon nanotube and graphene. *The Canadian Journal of Chemical Engineering*, *89*(6), 1342–1357. Retrieved from https://doi.org/10.1002/cjce.20586.

[40] **Tundwal, A., Kumar, H., Binoj, B. J., Sharma, R., Kumar, G., Kumari, R., Dhayal, A., Yadav, A., Singh, D., & Kumar, P.** (2024). Developments in conducting polymer-, metal oxide-, and carbon nanotube-based composite electrode materials for supercapacitors: a review. *RSC Advances*, *14*(14), 9406–9439. Retrieved from https://doi.org/10.1039/d3ra0831.

[41] **Olabi, A. G., Abbas, Q., Abdelkareem, M. A., Alami, A. H., Mirzaeian, M., & Sayed, E. T.** (2022). Carbon-Based Materials for supercapacitors: recent progress, challenges and barriers. *Batteries*, *9*(1), 19. Retrieved from https://doi.org/10.3390/batteries9010019.

[42] **Pal, B., Yang, S., Ramesh, S., Thangadurai, V., & Jose, R.** (2019). Electrolyte selection for supercapacitive devices: a critical review. *Nanoscale Advances*, *1*(10), 3807–3835. Retrieved from https://doi.org/10.1039/c9na00374f.

[43] **Zhong, C., Deng, Y., Hu, W., Qiao, J., Zhang, L., & Zhang, J.** (2015). A review of electrolyte materials and compositions for electrochemical supercapacitors. *Chemical Society Reviews*, *44*(21), 7484–7539. Retrieved from https://doi.org/10.1039/c5cs00303b.

[44] **Yu, L., & Chen, G. Z.** (2019). Ionic Liquid-Based electrolytes for supercapacitor and supercapattery. *Frontiers in Chemistry*, *7*. Retrieved from https://doi.org/10.3389/fchem.2019.00272.

[45] **Feng, Y., Liu, W., Wang, Y., Gao, W., Li, J., Liu, K., Wang, X., & Jiang, J.** (2020). Oxygen vacancies enhance supercapacitive performance of CuCo2O4 in high-energy-density asymmetric supercapacitors. *Journal of Power Sources*, *458*, 228005. Retrieved from https://doi.org/10.1016/j.jpowsour.2020.228005.

[46] **Xing, Z., Li, S., Wu, B., Wang, X., Wang, L., Wang, T., Liu, H., Zhang, M., Yun, D., Deng, L., Xie, S., Huang, R., & Zheng, L.** (2018). Photovoltaic performance and stability of fullerene/cerium oxide double electron transport layer superior to single one in p-i-n perovskite solar cells. *Journal of Power Sources*, *389*, 13–19. Retrieved from https://doi.org/10.1016/j.jpowsour.2018.03.079.

[47] **Käärik, M., Arulepp, M., Perkson, A., & Leis, J.** (2023). Effect of pore size distribution on energy storage of nanoporous carbon materials in neat and dilute ionic liquid electrolytes. *Molecules*, *28*(20), 7191. Retrieved from https://doi.org/10.3390/molecules28207191.

[48] **Dvoyashkin, M., Leistenschneider, D., Evans, J. D., Sander, M., & Borchardt, L.** (2021). Revealing the impact of hierarchical pore organization in supercapacitor electrodes by coupling ionic dynamics at micro- and macroscales. *Advanced Energy Materials*, *11*(24). Retrieved from https://doi.org/10.1002/aenm.202100700.

[49] **Zhao, L., Peng, Y., Dou, P., Li, Y., He, T., & Ran, F.** (2024). Surface chemistry of electrode materials toward improving electrolyte-wettability: A method review. *InfoMat*. Retrieved from https://doi.org/10.1002/inf2.12597.

[50] **Zhao, L., Li, Y., Yu, M., Peng, Y., & Ran, F.** (2023). Electrolyte-Wettability Issues and challenges of electrode materials in electrochemical energy storage, energy conversion, and beyond. *Advanced Science*, *10*(17). Retrieved from https://doi.org/10.1002/advs.202300283.

[51] **Li, Z., Lin, H., Ding, S., Ling, H., Wang, T., Miao, Z., Zhang, M., Meng, A., & Li, Q.** (2020). Synthesis and enhanced electromagnetic wave absorption performances of Fe3O4@C decorated walnut shell-derived porous carbon. *Carbon*, *167*, 148–159. Retrieved from https://doi.org/10.1016/j.carbon.2020.05.070.

[52] **Murthy, A. P., Madhavan, J., & Murugan, K.** (2018). Recent advances in hydrogen evolution reaction catalysts on carbon/carbon-based supports in acid media. *Journal of Power Sources*, *398*, 9–26. Retrieved from https://doi.org/10.1016/j.jpowsour.2018.07.040.

[53] **Song, M., Chen, K., & Wang, J.** (2019). A two-level approach for three-dimensional micro-siting optimization of large-scale wind farms. *Energy*, *190*, 116340. Retrieved from https://doi.org/10.1016/j.energy.2019.116340.

[54] **Czagany, M., Hompoth, S., Keshri, A. K., Pandit, N., Galambos, I., Gacsi, Z., & Baumli, P.** (2024b). Supercapacitors: an efficient way for energy storage application. *Materials*, *17*(3), 702. Retrieved from https://doi.org/10.3390/ma17030702.

[55] **Kumar, N., Kim, S., Lee, S., & Park, S**. (2022). Recent Advanced Supercapacitor: a review of storage mechanisms, electrode materials, modification, and perspectives. *Nanomaterials*, *12*(20), 3708. Retrieved from https://doi.org/10.3390/nano12203708.

[56] **Sahiner, N., & Sengel, S. B.** (2016). Quaternized polymeric microgels as metal free catalyst for H2 production from the methanolysis of sodium borohydride. *Journal of Power Sources*, *336*, 27–34. Retrieved from https://doi.org/10.1016/j.jpowsour.2016.10.054.

[57] **Sindhuja, M., Sudha, V., Abarna, M., & Harinipriya, S.** (2018). Electrochemical performance of Cu2+/Cu+ - [Fe(CN)6]3-/[Fe(CN)6]4- redox flow batteries under steady state conditions. *Electrochimica Acta*, *282*, 750–757. Retrieved from https://doi.org/10.1016/j.electacta.2018.06.124.

[58] **Bellos, E., Tzivanidis, C., & Tsifis, G.** (2017). Energetic, Exergetic, Economic and Environmental (4E) analysis of a solar assisted refrigeration system for various operating scenarios. *Energy Conversion and Management*, *148*, 1055–1069. Retrieved from https://doi.org/10.1016/j.enconman.2017.06.063.

[59] **Sánchez-Monreal, J., García-Salaberri, P. A., & Vera, M.** (2017). A genetically optimized kinetic model for ethanol electro-oxidation on Pt-based binary catalysts used in direct ethanol fuel cells. *Journal of Power Sources*, *363*, 341–355. Retrieved from https://doi.org/10.1016/j.jpowsour.2017.07.069.

[60] **Chang, Y., Chen, J., Qu, C., & Pan, T.** (2020). Intelligent fault diagnosis of Wind Turbines via a Deep Learning Network Using Parallel Convolution Layers with Multi-Scale Kernels. *Renewable Energy*, *153*, 205–213. Retrieved from https://doi.org/10.1016/j.renene.2020.02.004.

[61] **Ji, X., Liu, Y., Meng, J., & Wu, X.** (2020). Global supply chain of biomass use and the shift of environmental welfare from primary exploiters to final consumers. *Applied Energy*, *276*, 115484. Retrieved from https://doi.org/10.1016/j.apenergy.2020.115484.

[62] **Chen, J., Yang, L., Han, Y., Bao, Y., Zhang, K., Li, X., Pang, J., Chen, H., Song, W., Wei, Y., & Fang, D.** (2019). An in situ system for simultaneous stress measurement and optical observation of silicon thin film electrodes. *Journal of Power Sources*, *444*, 227227. Retrieved from https://doi.org/10.1016/j.jpowsour.2019.227227.

[63] **Abalyaeva, V., Efimov, M., Efimov, O., Karpacheva, G., Dremova, N., Kabachkov, E., & Muratov, D.** (2020). Electrochemical synthesis of composite based on polyaniline and activated IR pyrolyzed polyacrylonitrile on graphite foil electrode for enhanced

supercapacitor properties. *Electrochimica Acta*, *354*, 136671. Retrieved from https://doi.org/10.1016/j.electacta.2020.136671.

[64] **Li, S., He, W., Liu, B., Cui, J., Wang, X., Peng, D., Liu, B., & Qu, B.** (2019). One-step construction of three-dimensional nickel sulfide-embedded carbon matrix for sodium-ion batteries and hybrid capacitors. *Energy Storage Materials*, *25*, 636–643. Retrieved from https://doi.org/10.1016/j.ensm.2019.09.021.

[65] **Monama, G. R., Modibane, K. D., Ramohlola, K. E., Molapo, K. M., Hato, M. J., Makhafola, M. D., Mashao, G., Mdluli, S. B., & Iwuoha, E. I.** (2019b). Copper(II) phthalocyanine/metal organic framework electrocatalyst for hydrogen evolution reaction application. *International Journal of Hydrogen Energy*, *44*(34), 18891–18902. Retrieved from https://doi.org/10.1016/j.ijhydene.2019.02.052.

[66] **Gao, K., Gao, F., Li, J., He, C., Liu, M., Zhu, Q., Qian, Z., Ma, T., & Wang, P.** (2020). Biomimetic integrated olfactory sensory and olfactory bulb systems in vitro based on a chip. *Biosensors and Bioelectronics*, *171*, 112739. Retrieved from https://doi.org/10.1016/j.bios.2020.112739.

[67] **Zhang, Y., Wang, H., Sun, X., Wang, Y., & Liu, Z.** (2021). Separation and characterization of biomass components (cellulose, hemicellulose, and lignin) from corn stalk. *BioResources*, *16*(4), 7205–7219. Retrieved from https://doi.org/10.15376/biores.16.4.7205-7219.

[68] **Basu, P.** (2018). Introduction. In *Elsevier eBooks* (pp. 1–27). Retrieved from https://doi.org/10.1016/b978-0-12-812992-0.00001-7.

[69] **Mohan, D., Pittman, C. U., & Steele, P. H.** (2006). Pyrolysis of Wood/Biomass for Bio-oil: A Critical review. *Energy & Fuels*, *20*(3), 848–889. Retrieved from https://doi.org/10.1021/ef0502397.

[70] **Balat, M., & Ayar, G.** (2005b). Biomass Energy in the world, use of biomass and potential trends. *Energy Sources*, *27*(10), 931–940. Retrieved from https://doi.org/10.1080/00908310490449045.

[71] **Ghosh, S., Santhosh, R., Jeniffer, S., Raghavan, V., Jacob, G., Nanaji, K., Kollu, P., Jeong, S. K., & Grace, A. N.** (2019). Natural biomass derived hard carbon and activated carbons as electrochemical supercapacitor electrodes. *Scientific Reports*, *9*(1). Retrieved from https://doi.org/10.1038/s41598-019-52006-x.

[72] **Yang, H., Ye, S., Zhou, J., & Liang, T.** (2019). Biomass-Derived porous carbon materials for supercapacitor. *Frontiers in Chemistry*, *7*. Retrieved from https://doi.org/10.3389/fchem.2019.00274.

[73] **Zhu, Z., & Xu, Z.** (2020). The rational design of biomass-derived carbon materials towards next-generation energy storage: A review. *Renewable and Sustainable Energy Reviews*, *134*, 110308. Retrieved from https://doi.org/10.1016/j.rser.2020.110308.

[74] **Wang, J., Nie, P., Ding, B., Dong, S., Hao, X., Dou, H., & Zhang, X.** (2016). Biomass derived carbon for energy storage devices. *Journal of Materials Chemistry A*, *5*(6), 2411–2428. Retrieved from https://doi.org/10.1039/c6ta08742f.

[75] **Li, R., Zhou, Y., Li, W., Zhu, J., & Huang, W.** (2020). Structure engineering in Biomass-Derived carbon materials for electrochemical energy storage. *Research*, *2020*. Retrieved from https://doi.org/10.34133/2020/8685436.

[76] **Lu, H., & Zhao, X. S.** (2017). Biomass-derived carbon electrode materials for supercapacitors. *Sustainable Energy & Fuels*, *1*(6), 1265–1281. Retrieved from https://doi.org/10.1039/c7se00099e.

[77] **Scala, G., Delaval, M. N., Mukherjee, S. P., Federico, A., Khaliullin, T. O., Yanamala, N., Fatkhutdinova, L. M., Kisin, E. R., Greco, D., Fadeel, B., & Shvedova, A. A.** (2021). Multi-walled carbon nanotubes elicit concordant changes in DNA methylation and gene expression following long-term pulmonary exposure in mice. *Carbon*, *178*, 563–572. Retrieved from https://doi.org/10.1016/j.carbon.2021.03.045.

[78] **Zhang, W., Yin, J., Wang, C., Zhao, L., Jian, W., Lu, K., Lin, H., Qiu, X., & Alshareef, H. N.** (2021). Lignin derived porous carbons: synthesis methods and supercapacitor applications. *Small Methods*, *5*(11). Retrieved from https://doi.org/10.1002/smtd.202100896.

[79] **Assima, G. P., Dell'Orco, S., Navaee-Ardeh, S., & Lavoie, J.** (2017). Catalytic conversion of residual fine char recovered by aqueous scrubbing of syngas from urban biomass gasification. *Biomass and Bioenergy*, *100*, 98–107. Retrieved from https://doi.org/10.1016/j.biombioe.2017.03.015.

[80] **Rawat, S., Mishra, R. K., & Bhaskar, T.** (2021). Biomass derived functional carbon materials for supercapacitor applications. *Chemosphere*, *286*, 131961. Retrieved from https://doi.org/10.1016/j.chemosphere.2021.131961.

[81] **Jalal, N. I., Ibrahim, R. I., & Oudah, M. K.** (2021). A review on Supercapacitors: types and components. *Journal of Physics Conference Series*, *1973*(1), 012015. Retrieved from https://doi.org/10.1088/1742-6596/1973/1/012015.

[82] **Ricci, A., Olejar, K. J., Parpinello, G. P., Kilmartin, P. A., & Versari, A.** (2015). Application of fourier transform infrared (FTIR) spectroscopy in the characterization of tannins. *Applied Spectroscopy Reviews*, *50*(5), 407–442. Retrieved from https://doi.org/10.1080/05704928.2014.1000461.

[83] **Zhuang, J., Li, M., Pu, Y., Ragauskas, A., & Yoo, C.** (2020). Observation of potential contaminants in processed biomass using Fourier Transform infrared spectroscopy. *Applied Sciences*, *10*(12), 4345. Retrieved from https://doi.org/10.3390/app10124345.

[84] **Zhang, L. L., Zhou, R., & Zhao, X. S.** (2010). Graphene-based materials as supercapacitor electrodes. *Journal of Materials Chemistry*, *20*(29), 5983. Retrieved from https://doi.org/10.1039/c000417k.

[85] **Castro-Gutiérrez, J., Celzard, A., & Fierro, V.** (2020). Energy storage in supercapacitors: focus on Tannin-Derived carbon electrodes. *Frontiers in Materials*, *7*. Retrieved from https://doi.org/10.3389/fmats.2020.00217.

[86] **Potgieter-Vermaak, S., Maledi, N., Wagner, N., Van Heerden, J. H. P., Van Grieken, R., & Potgieter, J. H.** (2010). Raman spectroscopy for the analysis of coal: a review. *Journal of Raman Spectroscopy*, *42*(2), 123–129. Retrieved from https://doi.org/10.1002/jrs.2636.

[87] **Lee, S.-M.; Lee, S.-H.; Roh, J.-S.** Analysis of Activation Process of Carbon Black Based on Structural Parameters Obtained by XRD Analysis. Crystals 2021, 11, 153. Retrieved from https://doi.org/10.3390/cryst11020153.

[88] **Tian, Y., & Wu, J.** (2017). A comprehensive analysis of the BET area for nanoporous materials. AIChE Journal. Retrieved from https://doi.org/10.1002/aic.15880.

[89] **Yılmaz, A., Keshtiban, N. A., Gelir, A., Ozbek, N., Haykiri-Acma, H., & Yaman, S.** (2025). Rapeseed stalk-derived hierarchical porous carbon as electrode material for supercapacitors. *Industrial Crops and Products*, *226*, 120616. Retrieved from https://doi.org/10.1016/j.indcrop.2025.120616.

[90] **Aderyani, S., Flouda, P., Shah, S., Green, M., Lutkenhaus, J., & Ardebili, H.** (2021). Simulation of cyclic voltammetry in structural supercapacitors with pseudocapacitance behavior. *Electrochimica Acta*, *390*, 138822. Retrieved from https://doi.org/10.1016/j.electacta.2021.138822.

[91] **Hulicova-Jurcakova, D., Seredych, M., Lu, G. Q., & Bandosz, T. J.** (2008). Combined Effect of Nitrogen- and Oxygen-Containing Functional Groups of Microporous Activated Carbon on its Electrochemical Performance in Supercapacitors. *Advanced Functional Materials*, *19*(3), 438–447. Retrieved from https://doi.org/10.1002/adfm.200801236.

[92] **Licht, F., Davis, M., & Andreas, H.** (2019). Charge redistribution and electrode history impact galvanostatic charging/discharging and associated figures of merit. *Journal of Power Sources*, *446*, 227354. Retrieved from https://doi.org/10.1016/j.jpowsour.2019.227354.

[93] **Abid, M. a. '. M., Radzi, M. I., Mupit, M., Osman, H., Munawar, R. F., Samat, K. F., Suan, M. S. M., Isomura, K., & Islam, M. R.** (2020). Cyclic Voltammetry and Galvanostatic Charge-Discharge Analyses of Polyaniline/Graphene Oxide Nanocomposite based Supercapacitor. *Deleted Journal*, *3*(1), 14–26. Retrieved from https://doi.org/10.37934/mjcsm.3.1.1426.

[94] **Stoller, M. D., & Ruoff, R. S.** (2010). Best practice methods for determining an electrode material's performance for ultracapacitors. *Energy & Environmental Science*, *3*(9), 1294. Retrieved from https://doi.org/10.1039/c0ee00074d.

[95] **Simon, P., & Gogotsi, Y.** (2008). Materials for electrochemical capacitors. *Nature Materials*, *7*(11), 845–854. Retrieved from https://doi.org/10.1038/nmat2297.

CURRICULUM VITAE

Name Surname : Yaren Bumin

EDUCATION :

- **B.Sc. :** 2022, İstanbul Technical University, Faculty of Chemical and Metallurgical Engineering, Department of Chemical Engineering
- **M.Sc. :** 2025, İstanbul Technical University, Faculty of Chemical and Metallurgical Engineering, Department of Chemical Engineering

PROFESSIONAL EXPERIENCE AND REWARDS:

- 2019 Intern at BASF
- 2020 Intern at Philip Morris
- 2021 Long-term intern at Ford Otosan
- 2022 Program Purchaing Engineer at Ford Otosan
- 2024 Commodity Business Planner at Ford Otosan